

## Multiple origins of charnockite in the Mesoproterozoic Natal belt, Kwazulu-Natal, South Africa

G.H. Grantham<sup>a,\*</sup>, P. Mendonidis<sup>b</sup>, R.J. Thomas<sup>c</sup>, M. Satish-Kumar<sup>d</sup>

Four charnockite genetic models from the Natal belt are described, two of which have not previously been formally described in the literature.

New C isotope data indicate a mantle origin for the CO<sub>2</sub> inclusions previously reported from the magmatic charnockitic Port Edward Pluton.

1

# 1 **Multiple origins of charnockite in the Mesoproterozoic Natal belt,** 2 **Kwazulu-Natal, South Africa**

3  
4 **G.H. Grantham<sup>a,\*</sup>, P. Mendonidis<sup>b</sup>, R.J. Thomas<sup>c</sup>, M. Satish-Kumar<sup>d</sup>**

5  
6 <sup>a</sup> *Central Regions Unit, Council for Geoscience, P/Bag X112, Pretoria, South Africa*

7 <sup>b</sup> *Vaal University of Technology, Andries Potgieter Boulevard, Vanderbijlpark, South Africa*

8 <sup>c</sup> *British Geological Survey, Keyworth, Nottingham, NG12 5EQ, UK*

9 <sup>d</sup> *Institute of Geosciences, Faculty of Science, Shizuoka University, 836 Oya, Suruga-ku,*  
10 *Shizuoka, 422-8529, Japan*

11 \* corresponding author:

12 *Email address: grantham@geoscience.org.za*

13  
14 Received 1 December 2011; Received in revised form 20 April 2012; accepted 24 May 2012

15  
16 **Abstract** Four different varieties of charnockitic rocks, with different modes of formation, from  
17 the Mesoproterozoic Natal belt are described and new C isotope data presented. Excellent coastal  
18 exposures in a number of quarries and river sections make this part of the Natal belt a good  
19 location for observing charnockitic field relationships. Whereas there has been much debate on  
20 genesis of charnockites and the use of the term charnockite, it is generally recognized that the  
21 stabilization of orthopyroxene relative to biotite in granitoid rocks is a function of low  $a_{\text{H}_2\text{O}}$  ( $\pm$   
22 high  $\text{CO}_2$ ), high temperature, and composition (especially  $\text{Fe}/(\text{Fe}+\text{Mg})$ ). From the Natal belt  
23 exposures, it is evident that syn-emplacement, magmatic crystallization of charnockite can arise  
24 from mantle-derived differentiated melts that are inherently hot and dry (as in the Oribi Gorge

granites and Munster enderbite), as well as from wet granitic melts that have been affected through interaction with dry country rock to produce localized charnockitic marginal facies in plutons (as in the Portobello granite). Two varieties of post-emplacement sub-solidus charnockites are also evident. These include charnockitic aureoles developed in leucocratic, biotite, garnet granite adjacent to cross-cutting enderbitic veins that are attributed to metamorphic-metasomatic processes (as in the Nicholson's Point granite, a part of the Margate Granite Suite), as well as nebulous, patchy charnockitic veins in the Margate Granite that are attributed to anatexis metamorphic processes under low- $a_{\text{H}_2\text{O}}$  fluid conditions during a metamorphic event. These varieties of charnockite show that the required physical conditions of their genesis can be achieved through a number of geological processes, providing some important implications for the classification of charnockites, and for the interpretation of charnockite genesis in areas where poor exposure obscures field relationships.

Key Words: Charnockite igneous; Metamorphic; Natal belt; Dehydration  $\text{CO}_2$

## 1. Introduction

Charnockitic rocks are broadly defined as granitoids in terms of Quartz-Alkali feldspar-Plagioclase (QAP) ternary space but contain orthopyroxene (or fayalite + quartz) and, typically, perthite, mesoperthite or antiperthite (Le Maitre, 2002). Although not included in the formal definition, charnockitic rocks are typically characterized by meso- to melanocratic colour indices, being commonly described as having a "dark green, greasy" lustre and in contrast to the

leuco appearance normally expected of granitoids. The stabilization of orthopyroxene in granitic rocks and quartzofeldspathic granulites in high grade terrains essentially requires low  $a_{\text{H}_2\text{O}}$  and/or high temperatures typical of granulite grade environments. If  $a_{\text{H}_2\text{O}}$  is high, then typically orthopyroxene is replaced by biotite or amphibole, either in the solid state or as crystallizing phases in the melt at appropriate temperatures. The genesis of charnockitic rocks was widely debated during the 80's and 90's with numerous models revolving around the modes of genesis between magmatic and metamorphic varieties and the distinction of these (e.g. Bohlender et al., 1992) and particularly in the role of  $\text{CO}_2$  in the fluid phase (Newton et al., 1980; Friend, 1981; Janardhan et al., 1981; Kumar, 2004; Santosh and Omori, 2008; Huizenga and Touret, 2012; Touret and Huizenga, 2012). Carbon isotopic composition of fluid inclusions and graphite have served as distinct markers in identifying the mantle signatures of carbonic fluids in many occurrences of charnockite formation (e.g. Jackson et al., 1988; Farquhar and Chacko, 1991; Santosh et al., 1991; Luque et al., 2012).

A number of variations of these genetic models have been put forward over the years, including:

- Primary magmatic charnockite generated, with the crystallization of orthopyroxene, from high temperature magmas with low  $a_{\text{H}_2\text{O}}$  (Saxena, 1977; Martignole, 1979; Wickham, 1988; Stern and Dawoud, 1991; Kilpatrick and Ellis, 1992).
- Magmatic charnockite generated by the melting of granulites at high pressures in the presence of a carbon dioxide-rich fluid phase (Wendlandt, 1981).
- Metamorphic charnockites which are anhydrous restites of lower crust material from which partial melts have been removed (Fyfe, 1973; Newton and Hansen, 1983; Clemens, 1992).
- Metamorphic charnockites formed during granulite grade metamorphism under fluid

71 conditions of low oxygen fugacity and high partial pressures of carbon dioxide involving  
72 the breakdown of hydrous mafic phases and the generation of orthopyroxene (Janardhan  
73 et al., 1979; Newton et al., 1980; Friend, 1981; Hansen et al., 1984; Hansen et al., 1987;  
74 Hansen et al., 1995).

75 • Metasomatic charnockites formed by the dehydration of hydrous minerals by brines  
76 (Perchuk and Gerya, 1993; Aranovich and Newton, 1995).

77 • Metamorphic charnockites formed by thermal desiccation in aureoles adjacent to hot  
78 anhydrous intrusions emplaced into granitic rocks (van den Kerkhof and Grantham,  
79 1999).

80 Each of these mechanisms contributes to the fundamental requirements of high temperatures and  
81 low  $a_{\text{H}_2\text{O}}$  for charnockite genesis. However, since many of these examples occur in isolation, the  
82 interpreted mechanism was often extrapolated as the mechanism of formation of all charnockites,  
83 hence the debates. Many of the debates have since subsided with little resolution of the matter  
84 except to accept that multiple origins of orthopyroxene-bearing granitoid rocks are recognized.

85  
86 Charnockitic rocks from the southern portion of the Mesoproterozoic (ca. 1.2 to 1.0 Ga) Natal belt  
87 of KwaZulu-Natal, South Africa (Fig. 1), were first reported by Gevers (1941) and Gevers and  
88 Dunne (1942). The original mapping of this area was done by du Toit (1946) and later McIver  
89 (1963, 1966) provided a regional study of the area and described the major lithologies.  
90 Subsequently, we have recognized four distinct types of charnockite genesis in the area,  
91 comprising two magmatic and two metamorphic varieties. The description of these varieties and  
92 their interpreted genetic environments are the topic of this paper, supported by new C isotope data  
93 from some of the localities.

94

## 2. Natal Metamorphic Province

96

97 The Natal Metamorphic Province (“Natal belt” for short) consists of three tectonic terranes  
98 (Thomas, 1989; Fig. 1). A summary of the lithologies for which emplacement ages have been  
99 reported is depicted in Fig. 2, which shows that the Natal belt has a tectonomagmatic history  
100 spanning a period of time from >1200 Ma to ~1026 Ma. Geochemical data from lithologies from  
101 all three terranes (Thomas et al., 1994; Arima et al., 2001; Mendonidis et al., 2009) suggest  
102 island arc leading to the interpretation that the terranes were island arcs accreted onto the  
103 southern margin of the Archaean Kaapvaal Craton (Jacobs et al., 1993; Arima et al., 2001;  
104 McCourt et al., 2006).

105

106 The northernmost Tugela Terrane comprises plutonic, volcanic and sedimentary rocks that were  
107 obducted onto the southern margin of the Kaapvaal Craton, which they now overlie (Matthews,  
108 1972; Barkhuizen and Matthews, 1990; Johnston et al., 2003). The southern margin of the  
109 Tugela Terrane is marked by the Lilani-Matigulu shear zone (Thomas, 1989).

110

111 The Mzumbe Terrane covers a large area south of the Lilani-Matigulu shear zone, and comprises  
112 supracrustal gneisses, dated at ca. 1230 Ma (Thomas et al., 1999), which were intruded by a wide  
113 range of meta-igneous rocks including TTG orthogneisses and later gabbros (Thomas, 1989;  
114 Thomas and Eglington, 1990). The Mzumbe Terrane is separated from the southernmost Margate  
115 Terrane by the Melville thrust. The southernmost Margate Terrane consists of paragneisses  
116 intruded by calc-alkaline and tholeiitic, mafic to intermediate meta-igneous suites and a number

1  
2  
3  
4  
5  
6  
7  
8  
9  
10  
11  
12  
13  
14  
15  
16  
17  
18  
19  
20  
21  
22  
23  
24  
25  
26  
27  
28  
29  
30  
31  
32  
33  
34  
35  
36  
37  
38  
39  
40  
41  
42  
43  
44  
45  
46  
47  
48  
49  
50  
51  
52  
53  
54  
55  
56  
57  
58  
59  
60  
61  
62  
63  
64  
65

1  
2  
3 117 of granitic sheets and plutons (Talbot and Grantham, 1987). Large plutons of a rapakivi-  
4  
5  
6 118 charnockitic association collectively called the Oribi Gorge Suite (Thomas, 1988a, b; Thomas et  
7  
8  
9 119 al., 1993a; Grantham et al., 2001; Eglington et al., 2003) punctured both the Margate and  
10  
11 120 Mzumbe Terranes between 1090–1025 Ma (Fig. 2) indicating that these two terranes were  
12  
13 121 juxtaposed by that date (Thomas, 1989; Eglington et al., 2003; Eglington, 2006).

14  
15 122  
16  
17  
18 123 All three terranes experienced multiple deformational events and are characterized by pervasive  
19  
20 124 E-W trending fabrics and northward-verging overall structure (Talbot and Grantham, 1987;  
21  
22  
23 125 Mendonidis and Strydom, 1989; Thomas, 1989; Jacobs et al., 1993; McCourt et al., 2006;  
24  
25 126 Bisnath et al., 2008). However, the timing of the events in the different terranes was not coeval  
26  
27  
28 127 as shown in Fig. 2. Multiple metamorphic events have been reported from each terrane and  
29  
30 128 metamorphic textures suggest that metamorphism coincided with the deformation events  
31  
32  
33 129 (Mendonidis, 1989; Mendonidis et al., 2002; Mendonidis and Grantham, 2003; Bisnath et al.,  
34  
35 130 2008). Metamorphic grade generally increases from greenschist facies in the north to granulite  
36  
37  
38 131 facies in the south (Matthews, 1972; Thomas et al., 1994; McCourt et al., 2006).

39  
40 132  
41  
42 133 The earliest recognition and descriptions of charnockite in the Natal belt were by Gevers and  
43  
44  
45 134 Dunne (1942) and McIver (1963, 1966). Local, but excellent exposures, mostly above and in the  
46  
47  
48 135 intertidal zone along the coast, have facilitated the recognition of the various types of  
49  
50 136 charnockite described here, making the Natal Metamorphic Province an almost unique area to  
51  
52 137 study charnockite genesis, even by comparison with the classic charnockite areas of southern  
53  
54  
55 138 India.

### 56 57 139 **3. Magmatic charnockites**

58  
59  
60  
61  
62  
63  
64  
65



1  
2  
3 140  
4  
5  
6 141 The magmatic charnockites in the Natal belt are related to three distinct plutonic igneous rock  
7  
8 142 units: the Oribi Gorge Suite (OGS) (Thomas, 1988a, b; Thomas et al., 1991), the Munster Suite  
9  
10 143 (Mendonidis and Grantham, 1989, 1990) and the Margate Granite Suite (Thomas et al., 1991)  
11  
12 144 (Figs. 1 and 3). Within these intrusive suites, two charnockite varieties are distinguished based  
13  
14 145 on the dominant controlling factors of their genesis, namely fractionational crystallization and  
15  
16 146 fluid activity.  
17  
18  
19

20 147

### 23 148 *3.1 Charnockites with evidence of magmatic crystallization*

25 149

28 150 Two chemically distinct plutonic suites of megacrystic granitoids are recognized in the Natal belt  
29  
30 151 namely the Oribi Gorge Suite and the Munster Suite. The Oribi Gorge Suite contains the most  
31  
32 152 extensive development of charnockites in the Natal belt, where it is restricted to the Margate and  
33  
34 153 Mzumbe Terranes in the southern part of the belt (Thomas, 1988b, 1989; Fig. 1). The Oribi  
35  
36 154 Gorge Suite was intruded between ca. 1090 and 1025 Ma (Eglington et al., 2003). It is made up  
37  
38 155 of ten major plutons (up to 750 km<sup>2</sup> in extent), consisting of very coarse-grained, feldspar  
39  
40 156 porphyritic, locally rapakivi-textured, granitoid and charnockite. Eglington et al. (2003) provided  
41  
42 157 U-Pb SHRIMP ages for some of the plutons as follows: Two samples from the Oribi Gorge  
43  
44 158 plutons provided magmatic ages of  $1082 \pm 7$  Ma and  $1064 \pm 5$  Ma and a metamorphic rim age of  
45  
46 159  $1029 \pm 8$  Ma, and the Fafa and Port Edward plutons provided ages of  $1037 \pm 10$  Ma and  $1025 \pm$   
47  
48 160  $8$  Ma respectively. These data suggest two episodes of intrusion at  $\sim 1070$  and  $1030$  Ma  
49  
50 161 (Eglington et al., 2003). Intrusions in which charnockitic rocks are known to be developed  
51  
52 162 include the Port Edward, Oribi Gorge, Ntimbankulu, Fafa, KwaLembe, Mgeni and Glendale  
53  
54  
55  
56  
57  
58  
59  
60  
61  
62  
63  
64  
65

1  
2  
3  
4 163 plutons (Fig. 1). Some intrusions contain very little charnockite (e.g. the Mvenyane pluton),  
5  
6 164 whereas others are exclusively charnockitic (e.g. the Port Edward pluton). In the Oribi Gorge  
7  
8 165 Suite, a primary igneous flow fabric, formed by sub-parallel alignment of tabular feldspar  
9  
10 166 phenocrysts, can be seen locally in low-strain zones. Elsewhere, a weak to strong regional  $S_2$   
11  
12 167 fabric is developed, giving a pronounced gneissic foliation, especially around and parallel to  
13  
14 168 pluton margins where augen gneisses locally predominate. Pluton cores may contain low-strain  
15  
16 169 zones devoid of a tectonic fabric, though many are deformed by later ductile, transcurrent shears  
17  
18 170 which produced extensive, west-trending, sub-vertical augen gneiss and mylonite belts (Thomas,  
19  
20 171 1989; Thomas et al., 1991). The Oribi Gorge Granitoid Suite is characterized by megacrystic (up  
21  
22 172 to 6 cm) subhedral to euhedral feldspar grains with interstitial quartz, ferromagnesian and  
23  
24 173 accessory minerals (Fig. 4A). The ratio of K-feldspar and plagioclase is variable, so that within a  
25  
26 174 single pluton the normal granitic (charnockitic) composition grades to granodiorite (enderbite)  
27  
28 175 with increasing plagioclase, or monzonite/quartz monzonite (mangerite/mangeronorite) with  
29  
30 176 decreasing quartz. Rapakivi textures are locally recognizable in some plutons (Fig. 4C). The  
31  
32 177 Oribi Gorge charnockites (*sensu lato*) are typically very dark green to black in colour, have a  
33  
34 178 resinous lustre and consist of perthitic K-feldspar and/or antiperthitic plagioclase phenocrysts in  
35  
36 179 enderbite rocks. The coarse-grained groundmass is composed of quartz (8%–30%), antiperthitic  
37  
38 180 plagioclase ( $An_{25}$ ; 25%–60%) and subordinate microcline or orthoclase (12%–45% +  
39  
40 181 myrmekite). Mafic minerals, which form interstitial aggregates, include brown/brownish-green  
41  
42 182 hornblende (~5%), reddish-brown biotite (0–5%; locally symplectically intergrown with quartz),  
43  
44 183 weakly pleochroic orthopyroxene (5%–15%)  $\pm$  pale-green clinopyroxene (0–5%), partially  
45  
46 184 altered fayalite (0–5%) and late garnet (up to ~5%; commonly in garnet-quartz symplectite).  
47  
48 185 Accessory minerals include sulphides, ilmenite, zircon, apatite, allanite and graphite. Apatite,  
49  
50  
51  
52  
53  
54  
55  
56  
57  
58  
59  
60  
61  
62  
63  
64  
65

1  
2  
3 186 ilmenite and zircon commonly occur as inclusions in interstitial ferromagnesian minerals  
4  
5  
6 187 suggesting late crystallization. Olivine grains are locally mantled by orthopyroxene suggesting  
7  
8 188 the following reaction: fayalite + quartz  $\rightarrow$  orthopyroxene (Grantham et al., 2001).  
9

10 189  
11  
12  
13 190 The geochemistry from the various intrusions has been described and discussed in Grantham  
14  
15 191 (1984), Kerr (1985), Eglington et al. (1986), Thomas (1988b), Thomas and Mawson (1989) and  
16  
17  
18 192 Grantham et al. (2001). The Oribi Gorge Suite is typically tholeiitic with high FeO/(FeO+MgO  
19  
20 193 (Fig. 5) and shows A-type, within plate- and rapakivi-granite geochemical characteristics  
21  
22  
23 194 (Thomas, 1988b). K<sub>2</sub>O, Na<sub>2</sub>O, FeO and P<sub>2</sub>O<sub>5</sub> are high for average granitoids with comparable  
24  
25 195 silica contents. (Na<sub>2</sub>O+K<sub>2</sub>O)/CaO ratios, TiO<sub>2</sub> and P<sub>2</sub>O<sub>5</sub> contents are high. Trace element  
26  
27 196 abundances are also typical of A-type granitoids, with high contents of the HFS elements Nb, Y,  
28  
29  
30 197 Zr and Ba. Within individual plutons, major and trace element distributions show strong linear  
31  
32  
33 198 trends on Harker diagrams. The least evolved of the plutons, the Port Edward pluton has  
34  
35 199 marginal contact phases with relatively low SiO<sub>2</sub> contents of ~53% (Grantham, 1984), typical of  
36  
37 200 basic rocks, albeit with a high Fe/(Fe+Mg) ratio.  
38  
39

40 201  
41  
42 202 The geology and geochemistry of the Munster Suite has been described in detail by Mendonidis  
43  
44 203 and Grantham (1989, 1990) and has an age of ~1092 Ma (Mendonidis et al., 2009) indicating it  
45  
46  
47 204 is older than the Oribi Gorge Suite. The Munster Suite comprises older mafic granulites and  
48  
49  
50 205 younger intermediate charnockites. The older generation of coarse- to fine-grained, mafic rocks  
51  
52 206 contain plagioclase, two pyroxenes, biotite, minor K-feldspar  $\pm$  hornblende and quartz. The  
53  
54  
55 207 younger, coarse-grained charnockitic generation is quartz-monzonitic in composition and  
56  
57 208 consists of quartz, K-feldspar, plagioclase, orthopyroxene, clinopyroxene, biotite, opaque  
58  
59  
60  
61  
62  
63  
64  
65

1  
2  
3 209 mineral and apatite. These rocks are typically characterized by megacrystic (2–3 cm) plagioclase  
4  
5  
6 210 with interstitial quartz, ferromagnesian phases and accessory minerals, Mendonidis (1989)  
7  
8 211 recognized two generations of orthopyroxene in these rocks; an earlier magmatic variety and  
9  
10  
11 212 later metamorphic pyroxene derived from biotite and hornblende. The suite defines a calc-  
12  
13 213 alkaline trend and the rocks are characterized by high  $\text{TiO}_2$  and  $\text{P}_2\text{O}_5$  contents (Fig. 5).  
14  
15 214 Mendonidis and Grantham (1989) concluded that the basic and intermediate components of the  
16  
17  
18 215 Munster Suite were co-genetic.

19  
20 216  
21  
22  
23 217 Two pyroxene geothermometry on the basic rocks of the Munster Suite (after Lindsley, 1983),  
24  
25 218 using mineral core compositions, yielded magmatic temperatures of  $\sim 1050$  °C, whereas rim  
26  
27 219 compositions suggest far lower temperatures of  $\sim 600$  °C, reflecting metamorphic cooling or  
28  
29  
30 220 closure temperatures (Mendonidis and Grantham, 1989). This interpretation is supported by the  
31  
32  
33 221 occurrence of oscillatory zoning in clinopyroxene cores, interpreted as relict igneous features.  
34  
35 222 Conversely, no oscillatory zoning is seen in adjacent orthopyroxene, which is interpreted as a  
36  
37  
38 223 metamorphic rather than an igneous phase. Furthermore, petrographic textures indicate that  
39  
40 224 orthopyroxene developed at the expense of biotite and hornblende during prograde  
41  
42 225 metamorphism from amphibolite to granulite facies (Grantham, 1984).

43  
44 226  
45  
46  
47 227 Evidences for very high temperatures of  $\sim 1000$  °C in the Port Edward pluton of the Oribi Gorge  
48  
49  
50 228 Suite are derived from two pyroxene thermometry reported in Grantham et al. (2001). Saturation  
51  
52 229 surface thermometers based on the solubility studies of Zr and  $\text{P}_2\text{O}_5$  (Watson, 1979; Watson and  
53  
54  
55 230 Pabianco, 1981; Watson and Harrison, 1983) in granitic melts using available whole rock  
56  
57 231 chemistry (Grantham 1984; Mendonidis and Grantham, 1989) support high crystallization

1 11  
2  
3 232 temperatures.  $P_2O_5$  and Zr contents of the Port Edward pluton suggest temperatures of 1000–  
4  
5  
6 233 1050 °C and ~825–925 °C respectively whereas the data from the Munster Suite suggest  
7  
8 234 temperatures of 975–1025 °C and 825–850 °C respectively (Fig. 5). Similarly comparison of the  
9  
10 235  $TiO_2$  contents of these rock units with the solubility data of  $TiO_2$  of Green and Pearson (1986)  
11  
12 236 suggest temperatures of 1000–1050 °C and ~950 °C for the Port Edward pluton and Munster  
13  
14  
15 237 Suites respectively (Grantham et al., 2001 and Fig. 5).

16 238  
17  
18 239 Another group of rocks with magmatic charnockitic affinity is the Turtle Bay Suite, an undated  
19  
20  
21 240 meta-igneous association intruded along the tectonic boundary between the Mzumbe and  
22  
23 241 Margate terranes. The suite comprises a mantle-derived assemblage of mafic two-pyroxene  
24  
25 242 granulites and fractionated enderbites metamorphosed under granulite facies conditions of ca.  
26  
27 243 850 °C and ca. 6 kb (Thomas et al., 1992).

28  
29  
30 244  
31  
32 245 Radiogenic isotope data (Sm/Nd and Rb/Sr) indicate that the Oribi Gorge Suite is juvenile with  
33  
34  
35 246 Sm/Nd and Rb/Sr data showing no significant contributions from older crust (Eglington et al.,  
36  
37 247 1986; Grantham et al., 2001). No radiogenic isotope data are available from the Munster Suite.  
38  
39 248 Fluid inclusion studies on the Port Edward pluton reveal high density  $CO_2$  inclusions with  
40  
41 249 subordinate  $N_2$  and  $CH_4$  contents (Van der Kerkhof and Grantham, 1999).

42  
43 250  
44  
45 251 To further understand the genesis of these rocks and the source of the  $CO_2$ , which is present in  
46  
47 252 high levels in fluid inclusions (along with native graphite in the OGS charnockites) a carbon  
48  
49 253 isotope study was conducted on samples from the Port Edward and Oribi Gorge plutons. Sample  
50  
51 254 preparation and cleaning procedures followed the methods described in Miller and Pillinger  
52  
53  
54  
55  
56  
57  
58  
59  
60  
61  
62  
63  
64  
65

1  
2  
3 255 (1997). Bulk rock and mineral separates of 0.5 to 1 mm in size were hand-picked under a  
4  
5  
6 256 binocular microscope for the extraction of fluid inclusions by the heating method. Samples were  
7  
8 257 treated with hot 6 M HCl to remove any surficial carbonate contaminants and washed in distilled  
9  
10 258 water. Subsequently, the samples were ultrasonically cleaned in dichloromethane. Prior to  
11  
12  
13 259 extraction, 1 to 2 g of mineral separate was loaded into preheated (1100 °C, 12 h) 9 mm quartz  
14  
15 260 tubes and heated at 500 °C overnight to remove any surface and organic contaminants. An  
16  
17  
18 261 oxidizing agent (V<sub>2</sub>O<sub>5</sub>) was added to one aliquot each of bulk sample to check whether small  
19  
20 262 amounts of CH<sub>4</sub> or graphite are present, which can affect the isotopic composition (Satish-  
21  
22  
23 263 Kumar, 2005). The quartz tubes were then sealed under high vacuum and heated to 800 °C or  
24  
25 264 1000 °C and released gases were cryogenically purified and CO<sub>2</sub> was separated, and analyzed for  
26  
27  
28 265 its carbon isotope composition using a MAT-250 mass spectrometer at Shizuoka University,  
29  
30 266 Japan. CO<sub>2</sub> blanks during the heating experiments were always less than 0.005 mol.

31  
32  
33 267  
34  
35 268 The results of carbon isotopic composition of CO<sub>2</sub> extracted from fluid inclusions in two  
36  
37 269 representative samples are given in Table 2. The whole rock samples gave slightly lower  $\delta^{13}\text{C}$   
38  
39  
40 270 values at 1000 °C, when compared to those at 800 °C. This trend is again observed in CO<sub>2</sub>  
41  
42 271 extracted in samples with oxidizing agent, which implies that at 1000 °C there is a possibility that  
43  
44  
45 272 CO<sub>2</sub> was partly derived from the oxidation of small amounts of graphite. Graphite can be  
46  
47 273 deposited inside the fluid inclusions or in mineral grain boundaries during retrogression from  
48  
49  
50 274 CO<sub>2</sub>-rich fluids (e.g. Van der Kerkhof et al., 1991; Satish-Kumar, 2005; Papineau et al., 2010)  
51  
52 275 and is a primary constituent of some of the charnockites (Thomas, 1988b). Furthermore, minerals  
53  
54  
55 276 like quartz are vulnerable for secondary fluid inclusion entrapment and it is difficult to separate  
56  
57 277 primary and secondary fluid inclusions with heat extraction. The samples were pre-heated at 500  
58  
59  
60  
61  
62  
63  
64  
65

1  
2  
3 278 °C to decrepitate all possible low temperature secondary fluids. Therefore, the carbon isotopic  
4  
5  
6 279 composition of CO<sub>2</sub> extracted from fluid inclusions at 800 °C is considered as the best  
7  
8 280 approximate values for the fluid inclusions. The carbon isotopic composition of fluid inclusions  
9  
10 281 in both charnockite samples gave values comparable to mantle derived carbon (Table 2), which  
11  
12 282 is reported to have  $\delta^{13}\text{C}$  values around  $-5.5\text{‰}$  (Mattey, 1991; Deines, 2000). These values are  
13  
14  
15 283 also comparable with the fluid inclusion carbon isotope data described in southern Indian  
16  
17  
18 284 charnockite, which envisages a deep crustal or mantle source (e.g. Jackson et al., 1988; Santosh  
19  
20 285 et al., 1991). Significant differences between the quartz and whole rock values may reflect  
21  
22  
23 286 additional C bearing phases (carbonates?) in the whole rocks.  
24

25 287  
26  
27  
28 288 Recognizing the basic composition of some of the samples of the Oribi Gorge Suite (with SiO<sub>2</sub>  
29  
30 289 contents of <55% in, for example the Port Edward pluton) and the Munster Suite, their high  
31  
32 290 temperatures of crystallization of  $\sim 950\text{--}1050$  °C, indicated by two pyroxene thermometry and  
33  
34  
35 291 saturation surface thermometry, and the juvenile radiogenic and stable isotope data from the  
36  
37  
38 292 Oribi Gorge Suite, it is concluded that the magmas from which these rocks crystallized were  
39  
40 293 mantle derived. The original magmas were probably basaltic in origin. In the case of the Port  
41  
42 294 Edward pluton and probably the Oribi Gorge Suite in general, the magmas may have undergone  
43  
44  
45 295 two phases of crystallization with earlier crystallization at depth resulting in typical tholeiitic  
46  
47 296 Fe/(Fe+Mg) enrichment before emplacement and continued fractional crystallization at higher  
48  
49  
50 297 crustal levels. In contrast, basic members of the Munster Suite are recognized at the current  
51  
52 298 levels of exposure (Mendonidis and Grantham, 1989). The two suites are genetically distinct; the  
53  
54  
55 299 Oribi Gorge Suite including the Port Edward Pluton has Fe/(Fe+Mg) ratios of  $\sim 0.75$  and the  
56  
57 300 Munster Suite an Fe/(Fe+Mg) ratio of  $\sim 0.6$  (Figs. 5 and 6 in Grantham et al., 2001).  
58  
59  
60  
61  
62  
63  
64  
65

301  
302 The overall texture of the megacrystic charnockites of the Munster and Oribi Gorge Suites may  
303 also be interpreted in terms of experimental work by Wyllie et al. (1976) and Naney (1983),  
304 Whitney (1975) and Naney and Swanson (1980), who demonstrated that in granitic and  
305 granodioritic magmas, under conditions of reduced or low  $p(\text{H}_2\text{O})$  ( $w(\text{H}_2\text{O}) < 4.5\%$ ), plagioclase  
306 and alkali feldspar are early phases on the liquidus and commonly precede the crystallization of  
307 quartz and ferromagnesian phases (typically hornblende or orthopyroxene). In granodioritic  
308 systems with  $w(\text{H}_2\text{O}) > 4.5\%$ , on the other hand, hornblende is typically the first liquidus phase.  
309 Concomitant with low  $p(\text{H}_2\text{O})$  is the need for high magmatic temperatures of the order of  
310  $\sim 1000$  °C. The inferred crystallization path of these rocks is shown in Fig. 6. The path shows  
311 early crystallization of megacrystic plagioclase on the liquidus followed by orthopyroxene. Later  
312 as the K-feldspar field is crossed separate grains of orthoclase or as rapakivi overgrowths on  
313 plagioclase are formed with later interstitial or intercumulate orthopyroxene, opaque oxides and  
314 accessory phases zircon and apatite. The crystallization sequence will vary also due to changes in  
315 residual bulk composition with fractionation. The inferred crystallization sequence is reflected in  
316 Fig. 4B which shows a  $\sim 1$  cm plagioclase grain rimmed by quartz, ilmenite and poikilitic  
317 orthopyroxene and clinopyroxene grains, all of which contain inclusions of apatite and zircon.  
318 These inclusions indicate crystallization after the feldspars but preceding the pyroxene and  
319 ilmenite and imply near saturation of Zr,  $\text{P}_2\text{O}_5$  and  $\text{TiO}_2$  in the melt.

### 320 321 *3.2 Magmatic fluid activity charnockites in the Portobello Granite*

322 A second generation of leucocratic magmatic charnockites, with granitic (sensu stricto)  
323 composition, is recognized in the southern Margate Terrane of the Natal belt (Thomas, 1988a).



1  
2  
3 324 These charnockites are associated with non-charnockitic, often garnetiferous leucogranites. One  
4  
5  
6 325 body, the Portobello Granite shows both charnockitic and non-charnockitic facies. The non-  
7  
8 326 charnockitic variety is typically a red-coloured, biotite-chlorite granite exposed at the Portobello  
9  
10 327 headland and along Palm Beach (Figs. 3, 4d and 7) in which chlorite post-dates and mostly  
11  
12 328 replaces biotite, indicative of later, low-temperature alteration (Fig. 8a, b). There are also rare  
13  
14 329 chlorite grains which may be pseudomorphs after orthopyroxene, but no preserved  
15  
16 330 orthopyroxene has been recognized in the pink granite. Unequivocal contact relationships show  
17  
18 331 that the Portobello Granite intruded quartz monzonorites and metabasites of the Munster Suite  
19  
20 332 (Fig. 7). Wherever the granite is in contact with the quartz monzonorites, it is characterized by a  
21  
22 333 0.5 to 1.5 m wide grey-coloured, charnockitic marginal phase that contains biotite and  
23  
24 334 orthopyroxene as mafic phases (Figs. 4d and 8c, d). The charnockitic margins show a much  
25  
26 335 lower degree of chlorite alteration than the rest of the granite. A U-Pb zircon (SHRIMP)  
27  
28 336 discordant intercept age of  $1057 \pm 27$  Ma was determined for the main body of red-coloured  
29  
30 337 biotite-chlorite granite of the Portobello Granite from metamict zircon grains (Mendonidis and  
31  
32 338 Armstrong, 2009). The metamict nature of the zircons may be related to low temperature  
33  
34 339 alteration. Zircons from the charnockitic margins, on the other hand, produced a near-concordant  
35  
36 340 age of  $(1093 \pm 7)$  Ma that is statistically identical to the age of the adjacent Munster Suite quartz  
37  
38 341 monzonoritic country rocks ( $1091 \pm 7$  Ma) (Mendonidis and Armstrong, 2009; Mendonidis et al.,  
39  
40 342 2009). The zircons from the charnockitic margins were pristine, clear, transparent, light-brown  
41  
42 343 grains distinctly different from the milky, metamict grains of the rest of the granite, and  
43  
44 344 resembled those from the quartz monzonorites country rocks. Therefore, the zircons from the  
45  
46 345 charnockitic margins were interpreted as being xenocrysts derived from the partial assimilation  
47  
48 346 of the quartz monzonoritic country rocks (Mendonidis and Armstrong, 2009).  
49  
50  
51  
52  
53  
54  
55  
56  
57  
58  
59  
60  
61  
62  
63  
64  
65

1  
2  
3 347  
4  
5  
6 348 In comparison to the granite, the charnockitic margins are depleted in K, Rb, P, Y, Nb and REE,  
7  
8 349 and enriched in Ca, Ba and Sr (Mendonidis and Grantham, 2000, 2005; Table 3, Fig. 9). The  
9  
10 350 depletion of K and Rb in the marginal zones is inferred to be due to the migration of these  
11  
12 351 hydrophilic elements with the fluid into the country rock where they facilitated retrograde  
13  
14 352 alteration of orthopyroxene to biotite and/or to reduced crystallization of primary biotite in the  
15  
16 353 contact zone with Rb being typically strongly partitioned into K feldspar. The hydrous fluid may  
17  
18 354 also have fluxed melting reactions in the quartz monzonorite involving the breakdown of  
19  
20 355 plagioclase allowing partial assimilation, thus explaining the enrichment in Ca, Ba, and Sr in the  
21  
22 356 charnockitic margins. Phosphorous is relatively insoluble in felsic melts (Harrison and Watson,  
23  
24 357 1984) and may have precipitated and nucleated onto existing apatite in the country rock. The  
25  
26 358 depletion of Nb, Y and the REE can also be accounted for in terms of their being preferentially  
27  
28 359 partitioned into apatite in the quartz monzonoritic country rock.  
29  
30  
31  
32  
33  
34

35 360  
36  
37 361 An interpretation that accounts for all the observed features noted above is that the Portobello  
38  
39 362 Granite intruded as a wet felsic magma into the dry quartz monzonorite. On solidification, the  
40  
41 363 water that was dissolved in the melt remained as a hydrous fluid that promoted chloritic  
42  
43 364 alteration of the mafic phases in the granite. In the marginal zones, the fluid migrated along a  
44  
45 365 fluid gradient into the dry country rock, leaving the marginal zones relatively dry and thus  
46  
47 366 limiting retrograde alteration. This relationship is reflected in Fig. 10 in which the solidus curve  
48  
49 367 for wet granite is shown along with two curves for the dehydration reaction of  $Bt + Qtz \rightarrow Kfs +$   
50  
51 368  $Opx + H_2O$  with the two curves reflecting Mg and Fe end members (Mineral abbreviations after  
52  
53 369 Kretz, 1983). The two horizontally oriented arrows on Fig. 10 for the two curves show how with  
54  
55  
56  
57  
58  
59  
60  
61  
62  
63  
64  
65

17

370 a decreasing H<sub>2</sub>O fluid gradient, it would be possible to contribute to orthopyroxene  
371 crystallization/stabilization near the contact of the intrusion with dry country rock.

372

#### 373 4. Metamorphic charnockites

374

375 In addition to the charnockites which we interpret as of magmatic origin, as discussed above,  
376 two varieties of metamorphic charnockite, hosted in the Margate Granite Suite are recognized.  
377 The two types are further subdivided on the basis of the dominant controlling factor of their  
378 genesis namely, “thermal metamorphic charnockite” or “aureole charnockite” and “metamorphic  
379 fluid activity charnockite”.

380

##### 381 4.1 Thermal metamorphic charnockite (“aureole charnockite”)

382 This variety of charnockite is recognized in the Nicholson’s Point granite, a leucocratic biotite  
383 garnet granite and a member of the Margate Granite Suite, and has been described in detail by  
384 Grantham et al. (1996) and Van der Kerkhof and Grantham (1999). The critical exposures are  
385 seen at Nicholson’s Point (Fig. 11). At this locality the country rock Nicholson’s Point granite is  
386 intruded by veins of Port Edward Enderbite (Oribi Gorge Suite magmatic charnockite) up to ~10  
387 m thick as well as by pegmatitic veins up to ~30 cm wide. Adjacent to the veins of Port Edward  
388 enderbite, charnockitic aureoles with diffuse margins up to ~4 m wide are developed in the  
389 leucocratic biotite garnet Nicholson’s Point granite (Figs. 4A and 11). Aureoles in the granite  
390 adjacent to pegmatite veins are up to 0.5 m wide with aureole/vein width ratios ~10:1 (Fig. 4E)  
391 (Van der Kerkhof and Grantham, 1999).

392

1  
2  
3 393 The medium- to coarse-grained Nicholson's Point granite is a leucogranite composed of anhedral  
4  
5  
6 394 granoblastic orthoclase, plagioclase, quartz, biotite and garnet with accessory pyrite, ilmenite,  
7  
8 395 zircon and apatite. The charnockitic phase contains hypersthene (Fig. 8g, h), less biotite, but  
9  
10  
11 396 more plagioclase, myrmekite and opaque minerals relative to the granite. The sulphide in the  
12  
13 397 charnockite is pyrrhotite rather than pyrite. Garnet occurs both in the leucogranite and the  
14  
15 398 charnockite, either as euhedral to subhedral inclusion-free crystals (Fig. 8e, f) or as xenomorphic  
16  
17 399 poikilitic grains in symplectic intergrowth with quartz. The former generation is restricted to the  
18  
19  
20 400 granitic phase in which it occurs as isolated grains, commonly enclosed within feldspars and is  
21  
22  
23 401 interpreted as a primary igneous phase (Van der Kerkhof and Grantham, 1999). The garnet-  
24  
25 402 quartz symplectites occur adjacent to opaque minerals and around hypersthene in the  
26  
27 403 charnockitic phase and are interpreted to represent isobaric cooling reactions of  $\text{Opx/Mt} + \text{Pl} \rightarrow$   
28  
29  
30 404  $\text{Grt} + \text{Qtz}$  (Van der Kerkhof and Grantham, 1999). Where the two generations are in contact, the  
31  
32 405 symplectic garnet is seen to post-date the inclusion-free variety. Biotite is randomly distributed  
33  
34  
35 406 in the leucogranite, but occurs in association with mafic and opaque minerals in the charnockite.  
36  
37 407 This is interpreted as partial retrogressive hydration (Fig. 8g, h).  
38  
39

40 408  
41  
42 409 The same phenomenon is seen on a regional scale, where similar variations are observed  
43  
44 410 involving granites of the Margate Granite Suite comprising leucocratic pale grey to cream-  
45  
46 411 coloured garnetiferous granite with dark greyish green charnockite (Fig. 3; Thomas, 1988a;  
47  
48 Thomas et al., 1991) forming discontinuous, non-pervasive large-scale aureoles (> 1 km wide)  
49  
50 412 around plutons of the Oribi Gorge Suite (Fig. 3).  
51  
52 413  
53

54 414  
55  
56  
57  
58  
59  
60  
61  
62  
63  
64  
65

1  
2  
3 415 Thermobarometry and fluid inclusions studies were completed on the Nicholson's Point granite  
4  
5  
6 416 to investigate the causes of the charnockitisation. The minimum temperature conditions for the  
7  
8 417 charnockite forming reaction were constrained by the breakdown of pyrite to pyrrhotite at  
9  
10 418 ~700 °C, recognizing that the enderbite intruded with a temperature of ~900–1000 °C.  
11  
12  
13 419 Thermobarometry using compositional data from coexisting garnet and orthopyroxene yielded  
14  
15 420 lower unrealistic temperature estimates which were interpreted to represent cooling temperatures  
16  
17  
18 421 (Van der Kerkhof and Grantham, 1999).

19  
20 422  
21  
22  
23 423 Fluid inclusions studies of the rock units involved in this process showed that the intruding hot  
24  
25 424 Port Edward enderbite was characterized by dense CO<sub>2</sub> and N<sub>2</sub> fluid inclusions, the metamorphic  
26  
27 425 aureole by virtually pure H<sub>2</sub>O inclusions, whereas the country rock Nicholson's Point granite  
28  
29  
30 426 was characterized by saline H<sub>2</sub>O inclusions (Van der Kerkhof and Grantham, 1999). These  
31  
32 427 differences indicate that the charnockitic aureoles were not the result of CO<sub>2</sub> causing a reduction  
33  
34  
35 428 in the *a*H<sub>2</sub>O and stabilizing Opx and indicating a different mechanism for genesis. The densities  
36  
37 429 of the H<sub>2</sub>O-rich inclusions in the charnockite showed a wide range which was interpreted to  
38  
39  
40 430 reflect re-equilibration and implosion during the isobaric cooling path inferred in the area (Van  
41  
42 431 der Kerkhof and Grantham, 1999). In contrast, the CO<sub>2</sub> inclusions in the intruding enderbite  
43  
44  
45 432 showed a limited density range consistent with their entrapment at high temperatures of  
46  
47 433 crystallization. The survival of these inclusions was attributed to the isochores for CO<sub>2</sub> inclusions  
48  
49  
50 434 having shallower slopes and consequently being closer to the isobaric cooling path inferred for  
51  
52 435 the area (Van der Kerkhof and Grantham, 1999).

53  
54 436  
55  
56  
57  
58  
59  
60  
61  
62  
63  
64  
65

1  
2  
3 437 Even though the charnockitisation occurred at temperatures  $>700$  °C the Nicholson's Point  
4  
5  
6 438 granite country rock did not melt because it was virtually anhydrous. The granite contains only  
7  
8 439 ~5% biotite, containing a maximum of ~4% stoichiometric  $H_2O$ , so the amount of  $H_2O$  released  
9  
10 440 from the biotite breakdown reaction  $Bt + Qtz \rightarrow Opx + Kfs + H_2O$  was only ~0.2% of the rock by  
11  
12  
13 441 volume (Van der Kerkhof and Grantham, 1999). The effect of the low  $a_{H_2O}$  is summarized in  
14  
15  
16 442 Fig. 10. The vertical double-headed arrow on the figure defines the trajectory of the charnockite  
17  
18 443 forming reaction showing the crossing of the  $Bt + Qtz \rightarrow Opx + Kfs + H_2O$  reaction curve with  
19  
20 444 increasing temperature with the production of pyroxene in the solid state.  
21  
22

23 445  
24  
25 446 No significant differences are evident in the major element chemistry between the leucogranite  
26  
27  
28 447 and the charnockite phases of the Nicholson's Point granite, showing that the process is  
29  
30 448 essentially isochemical (Fig. 12). However, Grantham et al. (1996) noted that the charnockite is  
31  
32  
33 449 slightly depleted in Rb, Th, Nb, Y and REE (except Eu) whereas the charnockite is enriched in S,  
34  
35 450 Ba and Sr (Fig. 12).  
36

37 451  
38  
39  
40 452 The chemical variations are consistent with a combination of trace elements being incompatible  
41  
42 453 in the products of the charnockite-forming reaction and metasomatic introduction of mobile  
43  
44  
45 454 elements from the intruding magma. Depletions in the charnockite of Rb, Th, and Nb are  
46  
47 455 correlated with biotite being replaced by orthopyroxene whereas the REE depletions are  
48  
49  
50 456 correlated with the replacement of garnet by pyroxene recognizing that the REE are  
51  
52 457 preferentially partitioned into garnet and Rb, Th and Nb being preferentially partitioned into  
53  
54  
55 458 biotite (Grantham et al., 1996). The higher S, Ba and Sr are interpreted to be metasomatic  
56  
57 459 introductions from the enderbite.  
58  
59  
60  
61  
62  
63  
64  
65

1  
2  
3  
4 460  
5  
6 461 The discontinuous regional charnockite developed in the leucogranitic country rocks of the  
7  
8 462 Margate Granite Suite adjacent to magmatic charnockite intrusions thus probably represent  
9  
10 463 large-scale thermal aureoles in which biotite was dehydrated to form hypersthene and garnet was  
11  
12 464 altered to hypersthene. No  $p$ - $T$  studies have been done to understand the physical conditions with  
13  
14 465 such studies being dependant on identifying methods independent of fluid content and not  
15  
16 466 affected by subsolidus cooling and exchange. Charnockite aureoles adjacent to pegmatites show  
17  
18 467 identical geochemical features to those around enderbites. However, in view of the high  
19  
20 468 aureole/vein width ratio, they could not have developed as a result of high temperatures and it is  
21  
22 469 suggested that the charnockite-forming reaction in this case was fluid driven with the pegmatite  
23  
24 470 providing a sustained, possibly hypersaline, fluid source (Aranovich and Newton, 1995).  
25  
26  
27  
28  
29

30 471

#### 31 32 472 *4.2 Metamorphic fluid activity charnockite (fluid-induced charnockitisation)* 33 34

35 473  
36  
37 474 Vein-like and nebulous patches of coarse-grained charnockite have been described from southern  
38  
39 475 Natal (Thomas, 1988a). These resemble in appearance the well-documented “arrested  
40  
41 476 charnockites” of the Kerala region of southern India (e.g. Allen et al, 1985; Kumar, 2004; Raith  
42  
43 477 and Srikantappa, 2007) and like most of those, they post-date the metamorphic fabric and appear  
44  
45 478 to have originated by the introduction of fluids (Saunders, 1995).  
46  
47  
48  
49

50 479  
51  
52 480 In southern Natal, these charnockitic zones occur within the granite-gneisses of the Margate  
53  
54 481 Suite and Glenmore Granite, mostly in a wide belt around the southern margin of the Oribi  
55  
56 482 Gorge Pluton and close to the high-grade marbles of the Marble Delta Formation of the  
57  
58  
59  
60  
61  
62  
63  
64  
65

1 22  
2  
3 483 Mzimkulu Group (Thomas, 1988a; Fig. 3). The granites of both the Margate Suite and Glenmore  
4  
5  
6 484 Granite are strongly foliated and locally preserve evidence of two fabrics (Talbot and Grantham,  
7  
8 485 1987; Mendonidis and Strydom, 1989). They both have S-type chemical characteristics (  
9  
10 486 Mendonidis et al., 1991; Thomas et al., 1991) and may be interpreted as having originated by  
11  
12 487 fluid absent melting of metasediments (of the Mzimkulu Group?) during the high temperature-  
13  
14  
15 488 low pressure D1 (S1, M1) granulite event recognized by Mendonidis and Grantham (2003). Both  
16  
17  
18 489 these granites contain garnetiferous and charnockitic leucosomes that are concordant to the S2  
19  
20 490 fabric, and probably originated through syn-M2 fluid-absent anatexis (Saunders, 1995).  
21  
22  
23 491  
24  
25 492 Post-S2 vein and patch charnockites crop out at two quarries in the northern part of the Margate  
26  
27  
28 493 Terrane (Thomas, 1988a; Fig. 3). They are composed of typical, rather heterogeneous Margate  
29  
30 494 Suite garnet leucogranite and augen gneiss and are cut by a number of discordant charnockite  
31  
32 495 veins (Fig. 3; Thomas, 1988a). The charnockites in the two quarries were described in detail and  
33  
34  
35 496 interpreted by Saunders (1995). The distribution of the discordant pegmatitic charnockitic veins  
36  
37  
38 497 is controlled by small ductile shear zones with predominantly sinistral displacements. The host-  
39  
40 498 vein boundary is typically sharp and marked by a five-fold grain-size increase from ~0.5–2.5 mm  
41  
42 499 and a colour change from the light grey leucogranite to a typically charnockitic greenish-grey.  
43  
44  
45 500 The charnockitic veins have an unoriented igneous texture that almost, but not entirely,  
46  
47 501 obliterates the gneissic texture of the host rock (Fig. 4F), and there is no evidence of a chilled  
48  
49  
50 502 margin. They comprise randomly oriented subhedral megacrystic plagioclase, perthite,  
51  
52 503 micropertite and aggregates of fine-grained biotite, chlorite, calcite, dolomite and ilmenite  
53  
54  
55 504 which are pseudomorphic after orthopyroxene grains. Relative to the host gneisses, the  
56  
57 505 charnockitic veins are depleted in Fe, Mg, Mn, Ti, Ca, P, Nb, Zr, Y, U, Th, Ta, Sc and HREE,  
58  
59  
60  
61  
62  
63  
64  
65



506 and enriched in K, Ba, Sb, Pb, Sr, Rb and LREE. Si, Al and Na were immobile (Saunders, 1995;  
507 Fig. 13).

508  
509 The igneous textures of the charnockite veins indicate a super-solidus, i.e. melting, origin, but  
510 the lack of evidence for magmatic intrusion (e.g. local preservation of “ghost” foliation within  
511 the charnockite that is continuous from the country rock across the contact, see Fig. 4F) suggests  
512 that they were produced *in situ*. *In situ* fluid-absent melting of a biotite (hydrous phase) bearing  
513 gneiss can be initiated by an increase in temperature (>850 °C) or a decrease in pressure at high  
514 temperature through the breakdown of biotite by reaction with quartz to produce an anhydrous  
515 phase such as orthopyroxene or garnet which releases water that in turn fluxes a partial melt  
516 (Waters and Whales, 1984; Clemens, 1993; Stevens and Clemens, 1993; Vielzeuf and Montel,  
517 1994; Stevens et al., 1997). It is this anatexis process that was proposed for the origin of the  
518 concordant syn-D2 garnetiferous and charnockitic leucosomes by Saunders (1995). However, the  
519 post-D2 charnockitic veins are not associated with the regional metamorphic event as they are  
520 discordant to the regional tectonic fabric, and they do not display any of the typical migmatitic  
521 features such as mafic selvages of restitic material as seen in the syn-D2 leucosomes. Instead,  
522 their restriction to small sinistral faults favours a fluid-initiated melting process rather than a  
523 pervasive temperature increase. Saunders (1995) proposed that charnockitisation was a result of  
524 the introduction of partially hydrous (C-O-H) fluids under granulite facies conditions along  
525 structural dislocations. The introduction of such fluids would flux localized anatexis adjacent to  
526 the discontinuities to produce the pegmatitic charnockite veins. The water would be  
527 preferentially partitioned into the melt phase leaving behind a CO<sub>2</sub>-rich fluid, thus explaining the  
528 abundant CO<sub>2</sub> fluid inclusion within these charnockites. Moreover, the retrograde carbonate

alteration of the orthopyroxene can be ascribed to low temperature reaction with the remnant CO<sub>2</sub>-rich fluids. The small sinistral faults were probably produced during post-D2 uplift while the rocks were still hot (granulite facies). The origin of the carbonic (C-O-H) fluids could be related to granulite facies devolatilization of the nearby carbonate supracrustals of the Marble Delta Formation in the Margate Terrane (Fig. 3; Saunders, 1995). Alternatively, adjacent plutons of intruding Oriibi Gorge Suite which probably had CO<sub>2</sub> bearing fluids similar to those recorded in the Port Edward Pluton could have provided a source.

536

## 537 **5. Conclusions**

538

Exposures in the Mesoproterozoic Natal belt show four main types of charnockite formation and their inter-relationships. It thus constitutes an important area for studies of charnockite genesis on a par with, if not superior to, the classic southern India localities. The descriptions of the four varieties of charnockites from the Natal belt in this article show that orthopyroxene-bearing rocks with igneous textures can originate both from crystallization of dry, high-temperature, mantle-derived, differentiated mafic melts (magmatic charnockites), and by subsolidus metamorphic and metasomatic alteration of granitoid rocks at high temperatures and in the presence of fluids with low water activities (metamorphic charnockites). New C isotope data presented here show that the CO<sub>2</sub>-rich fluids associated with magmatic charnockites were mantle-derived. The origins of the metamorphic fluids involved in sub-solidus fluid related charnockitisation are not as well constrained, but field evidence suggests that these may have been introduced by intruding magmas and/or devolatilization of nearby carbonates during metamorphism. However, the distinction between magmatic and metamorphic charnockites can

25

552 be blurred as in the example of nebulous charnockitic veins of the Margate Suite Granite which  
553 have been interpreted as originating from *in situ*, post-emplacement, localized, fluid-induced  
554 melting (super-solidus charnockitisation) during later metamorphism. Moreover, the required  
555 low water activities in magmatic fluids need not be an inherent characteristic of the parent  
556 magmas but can also arise through interaction with country rock as in the case of the Portobello  
557 granite. The unequivocal field relationships and exposures in the Natal belt facilitate the clear  
558 distinction between magmatic and subsolidus charnockite genesis. In areas where such  
559 unequivocal exposures of orthopyroxene-bearing granitoid are absent, the uncertainty in  
560 recognizing whether the rocks are magmatic or metamorphic in origin has implications for the  
561 applicable nomenclature of such rocks, in view of a recent suggestion that the term charnockite  
562 should be reserved for those rocks clearly of magmatic origin (Frost and Frost, 2008). We do not  
563 subscribe to this view.

564

## 565 **Acknowledgments**

566

567 RJT thanks the CEO, NERC BGS for permission to publish. This paper is dedicated to John  
568 McIver who made the first detailed study of the charnockites of the Natal South Coast and who  
569 sadly passed away while it was being prepared. We would like to acknowledge constructive  
570 reviews by Dr. R. Voordouw and Dr. Lopamudra Saha. Samples with the prefix UND from the  
571 Port Edward pluton were analyzed from powders supplied to GHG by Bruce Eglington who is  
572 gratefully acknowledged.

573

574 **References**

- 575
- 576 Allen, P., Condie, K.C., Narayana, B.L., 1985. The geochemistry of prograde and retrograde  
577 charnockite-gneiss reactions in southern India. *Geochimica et Cosmochimica Acta* 49,  
578 323-336.
- 579 Aranovich, L.Y., Newton, R.C., 1995. Experimental determination of CO<sub>2</sub>-H<sub>2</sub>O activity-  
580 composition relations at 600–1000 °C and 6–14 kbar by reversed decarbonation and  
581 dehydration reactions. *American Mineralogist* 84, 1319-1332.
- 582 Arima, M., Tani, K., Kawate, S., Johnston, S.T., 2001. Geochemical characteristics and tectonic  
583 setting of metamorphosed rocks from the Tugela terrane, Natal belt, South Africa.  
584 *Memoirs of the National Institute of Polar Research Japan, Special Issue* 55, 1-39.
- 585 Barkhuizen, J.G., Matthews, P.E., 1990. Gravity modelling of the Natal Thrust Front: a Mid-  
586 Proterozoic crustal suture in southeastern Africa. *Geocongress'90 abstracts*, University of  
587 Cape Town, 32–35.
- 588 Bisnath, A., McCourt, S., Frimmel, H.E., Buthelezi, S.B.N., 2008. The metamorphic evolution of  
589 mafic rocks in the Tugela Terrane, Natal Belt, South Africa. *South African Journal of*  
590 *Geology* 111, 369-386.
- 591 Bohlender, F., van Reenen, D.D., Barton, J.M., 1992. Evidence for metamorphic charnockites in  
592 the southern Marginal Zone of the Limpopo Belt. *Precambrian Research* 55, 429-449.
- 593 Clemens, J.D., 1992. Partial melting and granulite genesis: A partisan overview. *Precambrian*  
594 *Research* 55, 297-301.
- 595 Clemens, J.D., 1993. Experimental evidence against CO<sub>2</sub>-promoted deep crustal melting. *Nature*  
596 363, 336-338.

- 1  
2  
3 597 Cornell, D.H., Thomas, R.J., 2006. Age and tectonic significance of the Banana Beach Gneiss,  
4  
5  
6 598 KwaZulu-Natal south coast, South Africa. *South African Journal of Geology* 109, 335-  
7  
8 599 340.  
9
- 10 600 Deines, P., 2000. The carbon isotope geochemistry of mantle xenoliths. *Earth Science Reviews*  
11  
12  
13 601 58, 247-278.  
14
- 15 602 Du Toit, A.L., 1946. The geology of parts of Pondoland, East Griqualand and Natal. Geological  
16  
17  
18 603 Survey of South Africa, Explanation Sheet 119.  
19
- 20 604 Ebadi, A., Johannes, W., 1991. Beginning of melting and components of first melts in the system  
21  
22  
23 605 Qz-Ab-Or-H<sub>2</sub>O-CO<sub>2</sub>. *Contributions to Mineralogy and Petrology* 106, 286-295.  
24
- 25 606 Eglinton, B.M., 2006. Evolution of the Namaqua-Natal Belt, southern Africa – A  
26  
27  
28 607 geochronological and isotope geochemical review. *Journal of African Earth Sciences* 46,  
29  
30 608 93-111.  
31
- 32 609 Eglinton, B.M., Harmer, R.E., Kerr, A., 1986. Petrographic, Rb-Sr isotope and geochemical  
33  
34  
35 610 characteristics of intrusive granitoids from the Port Edward - Port shepstone area, Natal.  
36  
37 611 *Transactions of the Geological Society of South Africa* 89, 199-213.  
38  
39
- 40 612 Eglinton, B.M., Thomas, R.J., Armstrong, R.A., Walraven, F., Kerr, A., Retief, E.A., 2003.  
41  
42 613 Zircon geochronology of the Oribi Gorge Suite, Kwa-Zulu Natal, South Africa:  
43  
44  
45 614 constraints on the timing of transcurrent shearing in the Namaqua-Natal Belt.  
46  
47 615 *Precambrian Research* 123, 29-46.  
48  
49
- 50 616 Eglinton, B.M., Thomas, R.J., Armstrong, R.A., 2010. U-Pb SHRIMP zircon dating of  
51  
52 617 Mesoproterozoic magmatic rocks from the Scottburgh area, central Mzumbe terrane,  
53  
54 618 KwaZulu-Natal, South Africa. *South African Journal of Geology* 113, 229-235.  
55  
56  
57  
58  
59  
60  
61  
62  
63  
64  
65

- 1  
2  
3 619 Farquhar, J., Chacko, T., 1991. Isotopic evidence for involvement of CO<sub>2</sub>-bearing magmas in  
4  
5  
6 620 granulite formation. *Nature* 354, 60-63.  
7  
8 621 Friend, C.R.L., 1981. Charnockite and granite formation and influx of CO<sub>2</sub> at Kabbaldurga.  
9  
10 622 *Nature* 294, 550-553.  
11  
12  
13 623 Frost, B.R., Frost, C.D., 2008. On charnockites. *Gondwana Research* 13, 30-44.  
14  
15 624 Fyfe, W.S., 1973. The granulite facies, partial melting and the Archaean crust. *Philosophical*  
16  
17  
18 625 *Transactions Royal Society London* A273, 457-461.  
19  
20 626 Gevers, T.W., 1941. Carbon dioxide and exhalations in northern Pondoland and Alfred County,  
21  
22  
23 627 Natal. *Transactions of the Geological Society of South Africa* 45, 223-301.  
24  
25 628 Gevers, T.W., Dunne, J.C., 1942. Charnockitic rocks near Port Edward in Alfred County, Natal.  
26  
27  
28 629 *Transactions of the Geological Society of South Africa* 45, 183-214.  
29  
30 630 Grantham, G.H., 1984. The tectonic, metamorphic and intrusive history of the Natal Mobile Belt  
31  
32  
33 631 between Glenmore and Port Edward, Natal. M.S. thesis, University of Natal  
34  
35 632 (Pietermaritzburg), 243pp.  
36  
37 633 Grantham, G.H., Allen, A.R., Cornell, D.H., Harris, C., 1996. Geology of Nicholson's point  
38  
39  
40 634 granite, Natal Metamorphic Province, South Africa: the chemistry of charnockitic  
41  
42  
43 635 alteration and origin of the granite. *Journal of African Earth Sciences* 23, 465-484.  
44  
45 636 Grantham, G.H., Eglinton, B.M., Thomas, R.J., Mendonidis, P., 2001. The nature of the  
46  
47  
48 637 Grenville-age Charnockitic A-type magmatism from the Natal, Namaqua and Maud Belts  
49  
50 638 of southern Africa and western Dronning Maud Land, Antarctica. *National Institute of*  
51  
52 639 *Polar Research, Tokyo, Special Issue* 55, 59-86.  
53  
54 640 Green, T.H., Pearson, N.J., 1986. Ti-rich accessory phase saturation in hydrous mafic-felsic  
55  
56  
57 641 compositions at high P, T. *Chemical Geology* 54, 185-201.  
58  
59  
60  
61  
62  
63  
64  
65

- 1  
2  
3  
4 642 Hansen, E.C., Janardhan, A.S., Newton, R.C., 1984. Fluid inclusions in rocks from the  
5  
6 643 amphibolite-facies to charnockite progression in southern Karnataka, India: Direct  
7  
8 644 evidence concerning the fluids of granulite metamorphism. *Journal of Metamorphic*  
9  
10 645 *Geology* 2, 249-264.
- 11  
12  
13 646 Hansen, E.C., Janardhan, A.S., Newton R.C., Prame, W.K.B.N., Ravindra, G.R., 1987. Arrested  
14  
15 647 charnockite formation in southern India and Sri Lanka. *Contributions to Mineralogy and*  
16  
17 648 *Petrology* 96, 225-244.
- 18  
19  
20 649 Hansen, E.C., Newton R.C., Janardhan, A.S., Lindeburg, S., 1995. Differentiation of late  
21  
22 650 Archaean crust in the eastern Dharwar Craton, Krishnagiri-Salem Area, south India.  
23  
24 651 *Journal of Geology* 103, 629-651.
- 25  
26  
27 652 Harrison, T.M., Watson, E.B., 1984. The behavior of apatite during crustal anatexis: Equilibrium  
28  
29 653 and kinetic considerations. *Geochimica et Cosmochimica Acta* 48, 1467-1477.
- 30  
31  
32 654 Holland, T.J.B., Powell, R., 1998. An internally consistent thermodynamic dataset for phases of  
33  
34 655 petrological interest. *Journal of Metamorphic Geology* 16, 309-343.
- 35  
36  
37 656 Huizenga, J.M., Touret, J.L.R., 2012. Granulites, CO<sub>2</sub> and graphite. *Gondwana Research*,  
38  
39 657 <http://dx.doi.org/10.1016/j.gr.2012.03.007>.
- 40  
41  
42 658 Irvine, T.N., Barager, W.R.A., 1971. A guide to the chemical classification of the common  
43  
44 659 volcanic rocks. *Canadian Journal of Earth Science* 8, 523-548.
- 45  
46  
47 660 Jackson, D.H., Matthey, D.P., Harris, N.B.W., 1988. Carbon isotope compositions of fluid  
48  
49 661 inclusions in charnockites from southern India. *Nature* 333, 167-170.
- 50  
51  
52 662 Jacobs, J., Thomas, R.J., Weber, K., 1993. Accretion and indentation tectonics at the southern  
53  
54 663 edge of the Kaapvaal craton during the Kibaran (Grenville) orogeny. *Geology* 21, 203-  
55  
56 664 206.
- 57  
58  
59  
60  
61  
62  
63  
64  
65

- 1  
2  
3 665 Janardhan, A.S., Newton, R.C., Smith, J.V., 1979. Ancient crustal metamorphism at low  $p\text{H}_2\text{O}$   
4  
5  
6 666 and charnockite formation at Kabbaldurga, South India. *Nature* 278, 511-514.  
7  
8 667 Janardhan, A.S., Newton, R.C., Hansen, E.C., 1982. The transformation of amphibolite facies  
9  
10 668 gneiss to charnockite in southern Karnataka and northern Tamil Nadu, India.  
11  
12  
13 669 *Contributions to Mineralogy and Petrology* 79, 130–149.  
14  
15 670 Johnston, S.T., Armstrong, R.A., Heaman, L., McCourt, S., Mitchell, A., Bisnath, A., Arima, M.,  
16  
17  
18 671 2001. Preliminary U-Pb geochronology of the Tugela Terrane, Natal Belt, eastern South  
19  
20 672 Africa. *Memoir National Institute of Polar Research, Special Issue* 55, 40-58.  
21  
22  
23 673 Johnston, S.T., McCourt, S., Bisnath, A., Mitchell, A.A., 2003. The Tugela Terrane, Natal Belt:  
24  
25 674 Kibaran magmatism and tectonism along the south eastern margin of the Kaapvaal Craton.  
26  
27  
28 675 *South African Journal of Geology* 106, 85-97.  
29  
30 676 Kerr, A., 1985. Characterization of the granitic rocks from the Valley of a Thousand Hills area,  
31  
32 677 Natal. *South African Journal of Science* 81, 475-478.  
33  
34  
35 678 Kilpatrick, J.A., Ellis, D.J., 1992. C-type magmas: Igneous charnockites and their extrusive  
36  
37 679 equivalents. *Transactions Royal Society Edinburgh: Earth Sciences* 83, 155-164.  
38  
39  
40 680 Kretz, R., 1983. Symbols for rock-forming minerals. *American Mineralogist* 68, 277-279.  
41  
42 681 Kumar, G.R.R., 2004. Mechanism of arrested charnockite formation at Nemmara, Palghat  
43  
44 682 region, southern India. *Lithos* 75, 331-358.  
45  
46  
47 683 Le Maitre, R.W., 2002. *Igneous Rocks: A Classification and Glossary of Terms*. Cambridge  
48  
49 684 University Press, New York, 236.  
50  
51  
52 685 Lindsley, D.H., 1983. Pyroxene thermometry. *American Mineralogist* 68, 477-493.  
53  
54  
55 686 Luque, F.J., Crespo-Feo, E., Barrenechea, J.G., Ortega, L., 2012. Carbon isotopes of graphite:  
56  
57 687 Implications on fluid history. *Geoscience Frontiers* 3, 197-207.  
58  
59  
60  
61  
62  
63  
64  
65



- 1  
2  
3 688 Martignole, J., 1979. Charnockite genesis and the Proterozoic crust. *Precambrian Research* 9,  
4  
5  
6 689 303-310.
- 7  
8 690 Matthews, P.E., 1972. Possible pre-Cambrian obduction and plate tectonics in southeastern  
9  
10 691 Africa. *Nature* 240, 37-39.
- 11  
12  
13 692 Matthey, D.P., 1991. Carbon dioxide solubility and carbon isotope fractionation in basaltic melt.  
14  
15 693 *Geochimica et Cosmochimica Acta* 55, 3467-3473.
- 16  
17  
18 694 McCourt, S., Armstrong, R.A., Grantham, G.H., Thomas, R.J., 2006. Geology and evolution of  
19  
20 695 the Natal Belt, South Africa. *Journal of African Earth Sciences* 46, 71-92.
- 21  
22  
23 696 McIver, J.R., 1963. A contribution to the Precambrian geology of southern Natal. PhD thesis,  
24  
25 697 University of Witwatersrand, 203pp.
- 26  
27  
28 698 McIver, J.R., 1966. Orthopyroxene-bearing granitic rocks from southern Natal. *Transactions of*  
29  
30 699 *the Geological Society of South Africa* 66, 99-117.
- 31  
32  
33 700 Mendonidis, P., Armstrong, R.A., Grantham, G.H., 2009. U-Pb SHRIMP ages and tectonic  
34  
35 701 setting of the Munster Suite of the Margate Terrane of the Natal Metamorphic Belt.  
36  
37 702 *Gondwana Research*, 15, 28-37.
- 38  
39  
40 703 Mendonidis, P., 1989. The tectonic evolution of a portion of the Southern Granulite Zone of the  
41  
42 704 Natal Mobile Belt, between Southbroom and Glenmore, Natal. PhD thesis, University of  
43  
44 705 Natal, Pietermaritzburg, 260 pp.
- 45  
46  
47 706 Mendonidis, P., Armstrong, R.A., Eglington, B.M., Grantham, G.H., Thomas, R.J., 2002.  
48  
49 707 Metamorphic history and U-Pb zircon (SHRIMP) geochronology of the Glenmore  
50  
51 708 Granite: implications for the tectonic evolution of the Natal Metamorphic Complex.  
52  
53  
54 709 *South African Journal of Geology* 105, 325-336.  
55  
56  
57  
58  
59  
60  
61  
62  
63  
64  
65

- 1  
2  
3 710 Mendonidis, P., Armstrong, R.A., 2009. A new U-Pb zircon age for the Portobello granite from  
4  
5  
6 711 the southern part of the Natal Metamorphic Belt. *South African Journal of Geology*, 112,  
7  
8 712 197-208.  
9
- 10 713 Mendonidis, P., Grantham, G.H., 2003. Petrology, origin and Metamorphic History of  
11  
12 714 Proterozoic-aged Granulites of the Natal Metamorphic province, southeastern Africa.  
13  
14 715 *Gondwana Research* 6, 607-628.  
15  
16 716 Mendonidis, P., Grantham, G.H., 1989. The distribution, petrology and geochemistry of the  
17  
18 717 Munster Suite, south coast, Natal. *South African Journal of Geology* 92, 377-388.  
19  
20  
21 718 Mendonidis, P., Grantham, G.H., 1990. Munster Suite. In: *Catalogue of South African*  
22  
23 719 *Lithostratigraphic Units* 2, 33-34.  
24  
25  
26 720 Mendonidis, P., Grantham, G.H., 2005. Geochemistry of the charnockitic marginal phase of the  
27  
28 721 portobello granite, natal metamorphic province. *GEO2005 Conference Abstracts*,  
29  
30 722 *Geological Society of South Africa, Durban*, p154-155.  
31  
32  
33 723 Mendonidis, P., Grantham, G.H., 2000. Rare earth element distribution and modelling in  
34  
35 724 charnockitic aureoles from southern Natal. *Journal of African Earth Sciences* 31, 51.  
36  
37  
38 725 Mendonidis, P., Strydom, D., 1989. Tectonic history of Proterozoic granulite gneisses between  
39  
40 726 Glenmore and Southbroom, southern Natal. *South African Journal of Geology* 92, 352-  
41  
42 727 368.  
43  
44  
45 728 Mendonidis, P., Grantham, G.H., Thomas, R.J., 1991. Glenmore Granite. In: Johnson, M.R.  
46  
47 729 (Ed.), *Catalogue of South African Lithostratigraphic Units*, South African Committee for  
48  
49 730 *Stratigraphy*, 13-14.  
50  
51  
52  
53  
54  
55  
56  
57  
58  
59  
60  
61  
62  
63  
64  
65

- 1  
2  
3 731 Miller, M.F., Pillinger, C.T., 1997. An appraisal of stepped heating release of fluid inclusion CO<sub>2</sub>  
4  
5  
6 732 for isotopic analysis: A preliminary to  $\delta^{13}\text{C}$  characterization of carbonaceous vesicles at  
7  
8 733 the nanomole level. *Geochimica et Cosmochimica Acta* 61, 193-205.  
9  
10 734 Naney, M.T., 1983. Phase equilibria of rock-forming ferromagnesian silicates in granitic  
11  
12 735 systems. *American Journal of Science* 283, 993-1033.  
13  
14  
15 736 Naney, M.T., Swanson, S.E., 1980. The effects of Fe and Mg on crystallisation in granitic  
16  
17 737 systems. *American Mineralogist* 65, 639-653.  
18  
19  
20 738 Newton, R.C., Smith, J.V., Windley, B.F., 1980. Carbonic metamorphism, granulites and crustal  
21  
22 739 growth. *Nature* 288, 45-50.  
23  
24  
25 740 Newton, R.C., Hanson, E.C., 1983. The origin of Proterozoic and late Archaean charnockites—  
26  
27 741 evidence from field relations and experimental petrology. In: Medaris, L.G., et al. (Eds.),  
28  
29 742 Proterozoic geology. *Geological Society of America Memoir* 161, p167-178.  
30  
31  
32 743 Papineau, D., De Gregorio, B.T., Cody, G.D., Fries, M.D., Mojzsis, S.J., Steele, A., Stroud,  
33  
34 744 R.M., Fogel, M.L., 2010. Ancient graphite in the Eoarchean quartz-pyroxene rocks from  
35  
36 745 Akilia in southern West Greenland I: Petrographic and spectroscopic characterization.  
37  
38 746 *Geochimica et Cosmochimica Acta* 74, 5862-5883.  
39  
40  
41 747 Purchuk, L.L., Gerya, T.V., 1993. Fluid control of charnockitisation. *Chemical Geology* 108,  
42  
43 748 175-186.  
44  
45  
46 749 Raith, M., Srikantappa, C., 2007. Arrested charnockite formation at Kottavattam, southern India.  
47  
48 750 *Journal of Metamorphic Petrology* 1196, 815-832.  
49  
50  
51 751 Santosh, M., Jackson, D.H., Harris, N.B.W., Matthey, D.P., 1991. Carbonic fluid inclusions in  
52  
53 752 South Indian granulites: evidence for entrapment during charnockite formation.  
54  
55 753 *Contributions to Mineralogy and Petrology* 108, 318-330.  
56  
57  
58  
59  
60  
61  
62  
63  
64  
65

- 1  
2  
3 754 Santosh, M., Omori, S., 2008. CO<sub>2</sub> windows from mantle to atmosphere: models on ultra-high  
4  
5  
6 755 temperature metamorphism and specifications on the link with melting of snowball Earth.  
7  
8 756 Gondwana Research 14, 82–96.  
9
- 10 757 Satish-Kumar, M., 2005. Graphite-bearing CO<sub>2</sub>-fluid inclusions in granulites: Insights on  
11  
12  
13 758 graphite precipitation and carbon isotope evolution. *Geochimica et Cosmochimica Acta*  
14  
15 759 69, 3841-3856.  
16  
17
- 18 760 Saunders, B., 1995. Fluid-induced charnockite formation post-dating prograde granulite facies  
19  
20 761 anatexis in southern Natal Metamorphic Province, South Africa. M.S. thesis, Rand  
21  
22  
23 762 Afrikaans University, 176 pp.  
24
- 25 763 Saxena, S.K., 1977. The charnockite geotherm. *Science* 198, 614-617.  
26  
27
- 28 764 Stern, R.J., Dawoud, A.S., 1991. Late Precambrian (740 Ma) charnockite, enderbite, and granite  
29  
30 765 from Jebel Moya, Sudan: A link between the Mozambique Belt and the Arabian-Nubian  
31  
32  
33 766 Shield? *Journal of Geology* 99, 648-659.  
34
- 35 767 Stevens, G., Clemens, J.D., 1993. Fluid-absent melting and the role of fluids in the lithosphere: a  
36  
37 768 slanted summary? *Chemical Geology* 108, 1-17.  
38  
39
- 40 769 Stevens, G., Clemens, J.D., Droop, G.T.R., 1997. Melt production during granulite facies  
41  
42 770 anatexis: experimental data from “primitive” metasedimentary protoliths. *Contributions*  
43  
44  
45 771 to *Mineralogy and Petrology* 128, 352-370.  
46
- 47 772 Talbot, C.J., Grantham, G.H., 1987. The Proterozoic intrusion and deformation of deep crustal  
48  
49  
50 773 ‘sills’ along the south coast of Natal. *South African Journal of Geology* 90, 520-538.  
51
- 52 774 Thomas, R.J., 1988a. The geology of the Port Shepstone area. Explanation of sheet 3030 Port  
53  
54  
55 775 Shepstone. Geological Survey of South Africa, Pretoria, 136pp.  
56  
57  
58  
59  
60  
61  
62  
63  
64  
65

- 1  
2  
3 776 Thomas, R.J., 1988b. The petrology of the Oribi Gorge Suite: Kibaran granitoids from southern  
4  
5  
6 777 Natal. *South African Journal of Geology* 91, 275-291.  
7  
8 778 Thomas, R.J., 1989. A tale of two tectonic terranes. *South African Journal of Geology* 92, 306-  
9  
10 779 321.  
11  
12  
13 780 Thomas, R.J., Mawson, S.A., 1989. Newly discovered outcrops of Proterozoic basement rocks in  
14  
15 781 northeastern Transkei. *South African Journal of Geology* 92, 369-376.  
16  
17  
18 782 Thomas, R.J., Eglington, B.M., 1990. A Rb-Sr, Sm-Nd and U-Pb zircon isotopic study of the  
19  
20 783 Mzumbe suite, the oldest intrusive granitoid in southern Natal, South Africa. *South*  
21  
22  
23 784 *African Journal of Geology* 93, 761-765.  
24  
25 785 Thomas, R.J., Mendonidis, P., Grantham, G.H., 1991. Margate Granite Suite. In: *Catalogue of*  
26  
27 786 *South African Lithostratigraphic Units* 3, 33-36.  
28  
29  
30 787 Thomas, R.J., 1991. Oribi Gorge Granitoid Suite. In: Johnson, M.R. (Ed.), *Catalogue of South*  
31  
32 788 *African lithostratigraphic units*. *South African Committee for Stratigraphy* 3, 37-40.  
33  
34  
35 789 Thomas, R.J., Ashwal, L., Andreoli, M.A.G., 1992. The Turtle Bay Suite: a mafic-felsic  
36  
37 790 granulite association from southern Natal, South Africa. *Journal of African Earth*  
38  
39  
40 791 *Sciences* 15(2), 187-206.  
41  
42 792 Thomas, R.J., Eglington, B.M., Bowring, S.A., Retief, E.A., Walraven, F., 1993a. New isotope  
43  
44 793 data from a Neoproterozoic porphyritic granitoid-charnockite suite from Natal, South  
45  
46  
47 794 Africa. *Precambrian Research* 62, 83-101.  
48  
49  
50 795 Thomas, R.J., Eglington, B.M., Bowring, S.A., 1993b. Dating the cessation of Kibaran  
51  
52 796 magmatism in Natal, South Africa. *Journal of African Earth Sciences* 16, 247-252.  
53  
54  
55 797 Thomas, R.J., Agenbacht, A.L.D., Cornell, D.H., Moore, J.M., 1994. The Kibaran of southern  
56  
57 798 Africa: Tectonic evolution and metallogeny. *Ore Geology Reviews* 9, 131-160.  
58  
59  
60  
61  
62  
63  
64  
65

- 1  
2  
3 799 Thomas, R.J., Cornell, D.H., Armstrong, R.A., 1999. Provenance age and metamorphic history  
4  
5  
6 800 of the Quha Formation, Natal Metamorphic Province: a U-Th-Pb zircon SHRIMP study.  
7  
8 801 South African Journal of Geology 102, 83-88.
- 10 802 Thomas, R.J., Armstrong, R.A., Eglington, B.M., 2003. Geochronology of the Sikombe Granite,  
11  
12 803 Transkei, Natal Metamorphic Province, South Africa. South African Journal of Geology  
13  
14 804 106, 403-408.
- 17 805 Touret, J.L.R., Huizenga, J.M., 2012. Fluid-assisted granulite metamorphism: A continental  
18  
19 806 journey. Gondwana Research 21, 224-235.
- 22 807 Van der Kerkhof, A.M., Grantham, G.H., 1999. Metamorphic charnockite in contact aureoles  
23  
24 808 around intrusive enderbite from Natal. Contributions to Mineralogy and Petrology 137,  
25  
26 809 115-132.
- 29 810 Van den Kerkhof, A.M., Touret, J.L.R., Maijer, C., Jensen, J.B.H., 1991. Retrograde methane  
30  
31 811 dominated fluid inclusions from high-temperature granulites of Rogaland, southwestern  
32  
33 812 Norway. Geochimica et Cosmochimica Acta 55, 2533-2544.
- 36 813 Vielzuef, D., Montel, J.M., 1994. Partial melting of metagreywackes. Part 1. Fluid absent  
37  
38 814 experiments and phase relationships. Contributions to Mineralogy and Petrology 117,  
39  
40 815 375-393.
- 43 816 Waters, D.J., Whales, C.J., 1984. Dehydration melting and the granulites transition in  
44  
45 817 metapelites from southern Namaqualand, S. Africa. Contributions to Mineralogy and  
46  
47 818 Petrology 88, 269-275.
- 50 819 Watson, E.B., 1979. Zircon saturation in felsic liquids: Experimental results and applications to  
51  
52 820 trace element chemistry. Contributions to Mineralogy and Petrology 70, 407-419.  
53  
54  
55  
56  
57  
58  
59  
60  
61  
62  
63  
64  
65

- 1  
2  
3 821 Watson, E.B., Capobiano, C.J., 1981. Phosphorous and the rare earth elements in felsic magmas:  
4  
5  
6 822 an assessment of the role of apatite. *Geochemica et Cosmochemica Acta* 45, 2349-2358.  
7  
8 823 Watson, E.B., Harrison, T.M., 1983. Zircon saturation revisited: temperature and composition  
9  
10 824 effects in a variety of crustal magma types. *Earth and Planetary Science Letters* 64, 295-  
11  
12 304.  
13 825  
14  
15 826 Wentlandt, R.F., 1981. Influence of CO<sub>2</sub> on melting of model granulite facies assemblages: A  
16  
17  
18 827 model for the genesis of charnockites. *American Mineralogist* 66, 1164-1174.  
19  
20 828 Whitney, J.A., 1975. The effects of pressure and X<sub>H<sub>2</sub>O</sub> on phase assemblages in four synthetic  
21  
22  
23 829 rock compositions. *Journal of Geology* 83, 1-32.  
24  
25 830 Wickham, S.M., 1988. Evolution of the lower crust. *Nature* 333, 119-120.  
26  
27  
28 831 Wyllie, P.J., Huang, W., Stern, C.R., Maaloe, S., 1976. Granitic magmas: possible and  
29  
30 832 impossible sources, water contents and crystallization sequences. *Canadian Journal Earth*  
31  
32  
33 833 *Science* 13, 1007-1019.  
34  
35 834  
36  
37  
38  
39  
40  
41  
42  
43  
44  
45  
46  
47  
48  
49  
50  
51  
52  
53  
54  
55  
56  
57  
58  
59  
60  
61  
62  
63  
64  
65

## 835 Figure Captions

836

837 Figure 1 Locality map of southern Natal Metamorphic Province showing other locality maps and  
838 distribution of the Oribi Gorge Suite.

839

840 Figure 2 Graphical tabulation of the Natal Metamorphic belt lithologies for which there are  
841 published emplacement ages, sorted according to the age scale on the left (After Mendonidis and  
842 Armstrong, 2009). Superscripts refer to the source of the age as follows: <sup>1</sup> Johnston et al., 2001; <sup>2</sup>  
843 Thomas et al., 1999; <sup>3</sup> Thomas and Eglington, 1990; <sup>4</sup> Eglington et al., 2010; <sup>5</sup> Eglington et al.,  
844 2003; <sup>6</sup> Mendonidis et al., 2002; <sup>7</sup> Mendonidis et al., 2009; <sup>8</sup> Mendonidis and Armstrong, 2009; <sup>9</sup>  
845 Cornell and Thomas, 2006; <sup>10</sup> Thomas et al., 1993; <sup>11</sup> Thomas et al., 2003; The Sikombe Granite  
846 occurs to the south of the Margate Terrane and may or may not be part of a separate block  
847 (Thomas et al., 2003). The shaded blocks indicate lithologies that contain charnockitic rocks.

848

849 Figure 3 Locality map of Margate Terrane showing the distribution of Munster Suite and other  
850 charnockite varieties including the Oribi Gorge Suite and the Margate Granite thermal aureoles  
851 and fluid gradient charnockites. Also shown are the locations of detailed maps shown in Figs. 7  
852 and 10. Note also the location of Marble Delta as well as the quarry location where fluid-driven  
853 charnockites are exposed.

854

855 Figure 4 Photos of various charnockite localities from Natal. (A) The contact zone between the  
856 Oribi Gorge Suite (OGS) (Port Edward pluton) and Margate Suite (Nicholson's Point granite,  
857 NPG) at Nicholson's Point showing the megacrystic OGS at left. The first 30–40 cm of NPG  
858 from the contact is opx-bearing whereas the rest of the NPG has garnet and biotite; (B) Thin  
859 section micrograph in plane polarised light of the OGS showing porphyritic plagioclase rimmed  
860 by intercumulate quartz, ilmenite and poikilitic pyroxene containing inclusions of apatite and  
861 zircon. The field of view is 10 mm; (C) Rapakivi texture in the OGS; (D) Photograph of the  
862 contact zone between the Munster Suite (at left), the marginal orthopyroxene zone and the pink  
863 Portobello granite at Palm Beach; (E) Charnockitic aureole developed adjacent to a pegmatitic  
864 quartz vein intruding the Nicholsons Point granite (Margate Suite) at Nicholsons Point; (F)

1  
2  
3  
4  
5  
6  
7  
8  
9  
10  
11  
12  
13  
14  
15  
16  
17  
18  
19  
20  
21  
22  
23  
24  
25  
26  
27  
28  
29  
30  
31  
32  
33  
34  
35  
36  
37  
38  
39  
40  
41  
42  
43  
44  
45  
46  
47  
48  
49  
50  
51  
52  
53  
54  
55  
56  
57  
58  
59  
60  
61  
62  
63  
64  
65



1  
2  
3 865 Charnockite vein (right) in the garnet biotite bearing Margate Suite at left. The pegmatitic vein  
4  
5 866 intruding the Margate Suite is traceable through the charnockite vein indicating the metamorphic  
6  
7 867 origin of the charnockite. The dark coarse crystals in the charnockite zone are porphyroblastic  
8  
9 868 orthopyroxene.

10  
11 869  
12  
13 870 Figure 5 (A) AFM diagram after Irvine and Barager (1971) showing the difference in Fe/(Fe+Mg)  
14  
15 871 between the Munster Suite (MS) and the Oribi Gorge Suite (PE); (B) Saturation surface  
16  
17 872 thermometry using the Zr and P<sub>2</sub>O<sub>5</sub> contents of the Port Edward pluton of the Oribi Gorge Suite  
18  
19 873 (PE) and the Munster Suite (MS); (C) Comparison of the TiO<sub>2</sub> contents of the Port Edward  
20  
21 874 pluton of the Oribi Gorge Suite (PE) and the Munster Suite (MS) with saturation curves at  
22  
23 875 various temperatures after Green and Pearson (1986).

24 876  
25 877 Figure 6 Interpreted crystallization sequence for the Port Edward pluton of the Oribi Gorge Suite  
26  
27 878 and the Munster Suite, modified after Naney (1983) and Naney and Swanson (1980).

28  
29 879  
30  
31 880 Figure 7 Detailed geological map of the charnockitic zones adjacent to the Munster Suite at Palm  
32  
33 881 Beach. Note the development of the charnockitic Margate Suite adjacent to the quartz  
34  
35 882 monzonitic Munster Suite.

36 883  
37  
38 884 Figure 8 Thin section photographs from the Portobello granite (A, B, C and D) and the  
39  
40 885 Nicholsons's Point granite. Field of view is ~3 mm with plane polarised light images at left and  
41  
42 886 crossed polar images at right. A–B: Photomicrographs from the chlorite bearing Portobello  
43  
44 887 granite. Note also the more altered feldspars; C–D: Photomicrographs from the charnockitic  
45  
46 888 Portobello granite; E–F: Photomicrographs from the garnet+biotite bearing Nicholsons Point  
47  
48 889 granite. Note the inclusion free subhedral garnet inferred to be of igneous origin; G–H:  
49  
50 890 Photomicrographs from the charnockitic Nicholsons's Point granite.

51 891  
52  
53 892 Figure 9 Plot of whole rock chemistry of charnockitic marginal zones of the Portobello granite  
54  
55 893 normalized against the host biotite chlorite granite. Data from Mendonidis and Grantham  
56  
57 894 (unpublished). The marked depletion in yttrium and niobium is probably because the distribution  
58  
59 895 and migration of these elements is largely controlled by accessory phosphate phases that are

60  
61  
62  
63  
64  
65

1  
2  
3 896 relatively insoluble in felsic liquids. Clear enrichment in Ca, Ba and Sr is evident in the  
4  
5 897 charnockitic Portobello granite, which is probably due to assimilation of country rock  
6  
7 898 plagioclase.

8  
9 899  
10  
11 900 Figure 10  $T$ - $X_{\text{H}_2\text{O}}$  diagram for the wet granite solidus after Ebadi and Johannes (1991) and two  
12  
13 901 dehydration reaction curves for quartz plus annite (Fe) and phlogopite (Mg) to form  
14  
15 902 orthopyroxene and K feldspar (in the melt) at 5 kb. The reaction curves were calculated using  
16  
17 903 THERMOCALC (Holland and Powell, 1998). The horizontal arrows show the effect of a  
18  
19 904 decreasing fluid gradient inferred to have assisted the crystallization of orthopyroxene in the  
20  
21 905 contact zone applicable to the Portobello Granite at Palm Beach. The vertical double-headed  
22  
23 906 arrow shows the thermal dessication effect of heating by adjacent intrusions resulting in contact  
24  
25 907 metamorphic charnockitic aureoles as seen at Nicholson's Point.

26  
27 908  
28  
29 909 Figure 11 Geological map of Nicholson's Point showing the development of charnockite in  
30  
31 910 aureoles adjacent to Port Edward enderbite of the Oribi Gorge Suite as well adjacent to thin  
32  
33 911 pegmatite veins.

34  
35 912  
36  
37 913 Figure 12 Plot of whole rock chemistry of charnockitic aureoles normalized against the mean of  
38  
39 914 the garnet biotite granite from Nicholson's Point Granite at Nicholson's Point. Data from  
40  
41 915 Grantham et al. (1996).

42 916  
43  
44 917 Figure 13 Plot of whole rock chemistry of post-D2 charnockitic veins normalized against the  
45  
46 918 immediate host rocks, from the Mzimkulu and Beacon Lot quarries. Data from Saunders (1995).

47  
48  
49  
50  
51  
52  
53  
54  
55  
56  
57  
58  
59  
60  
61  
62  
63  
64  
65

Figure 1

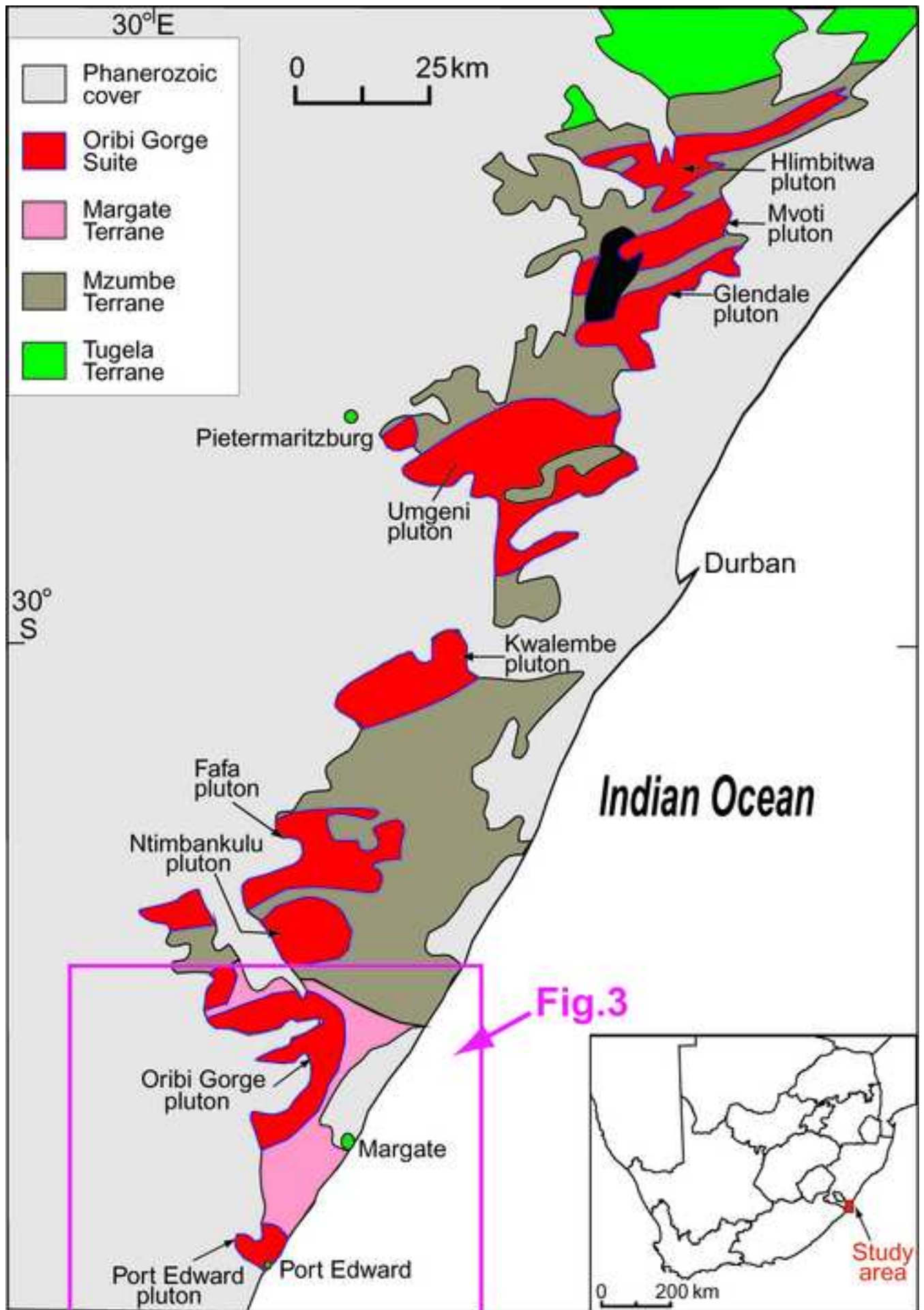


Figure 2

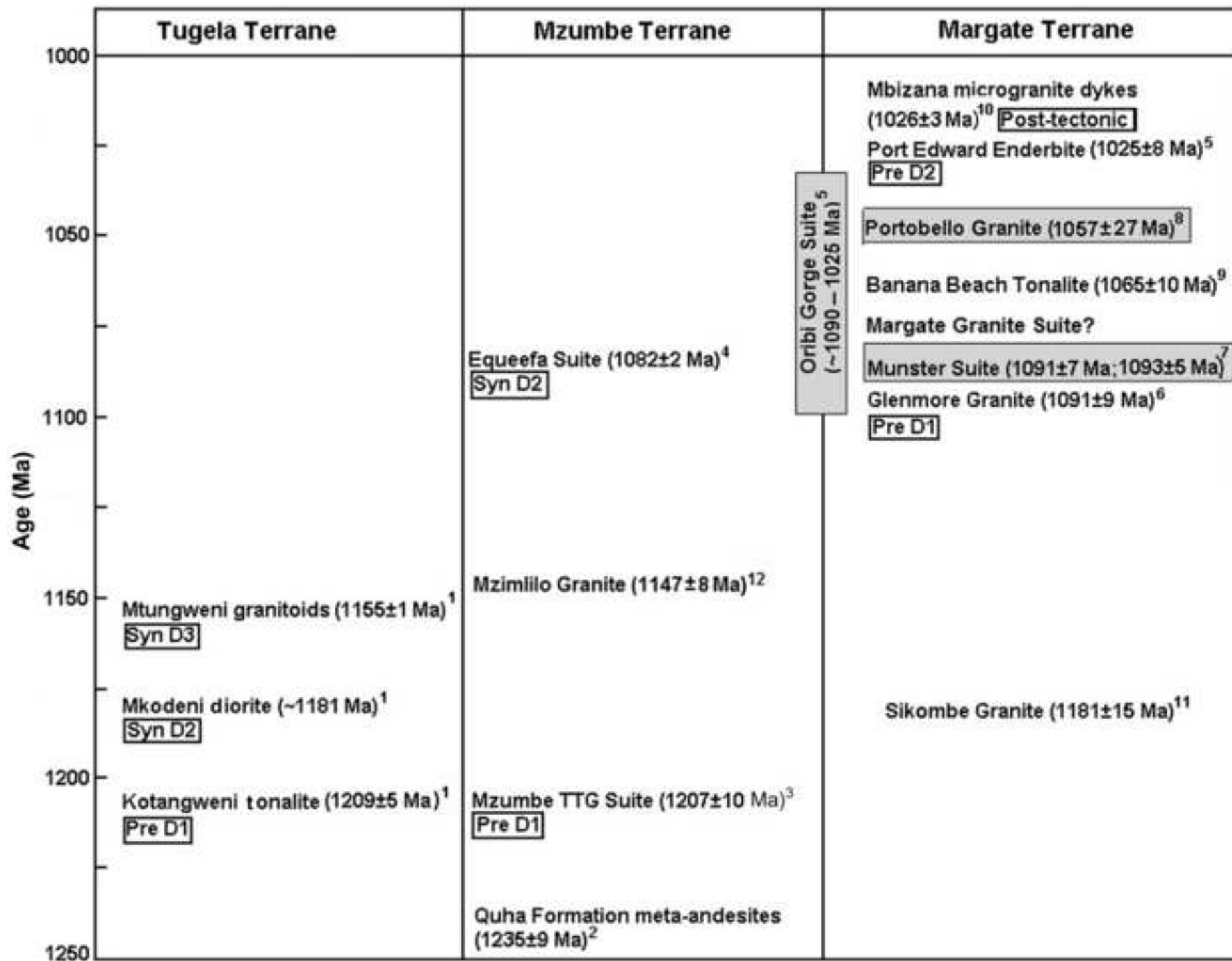
[Click here to download high resolution image](#)

Figure 3

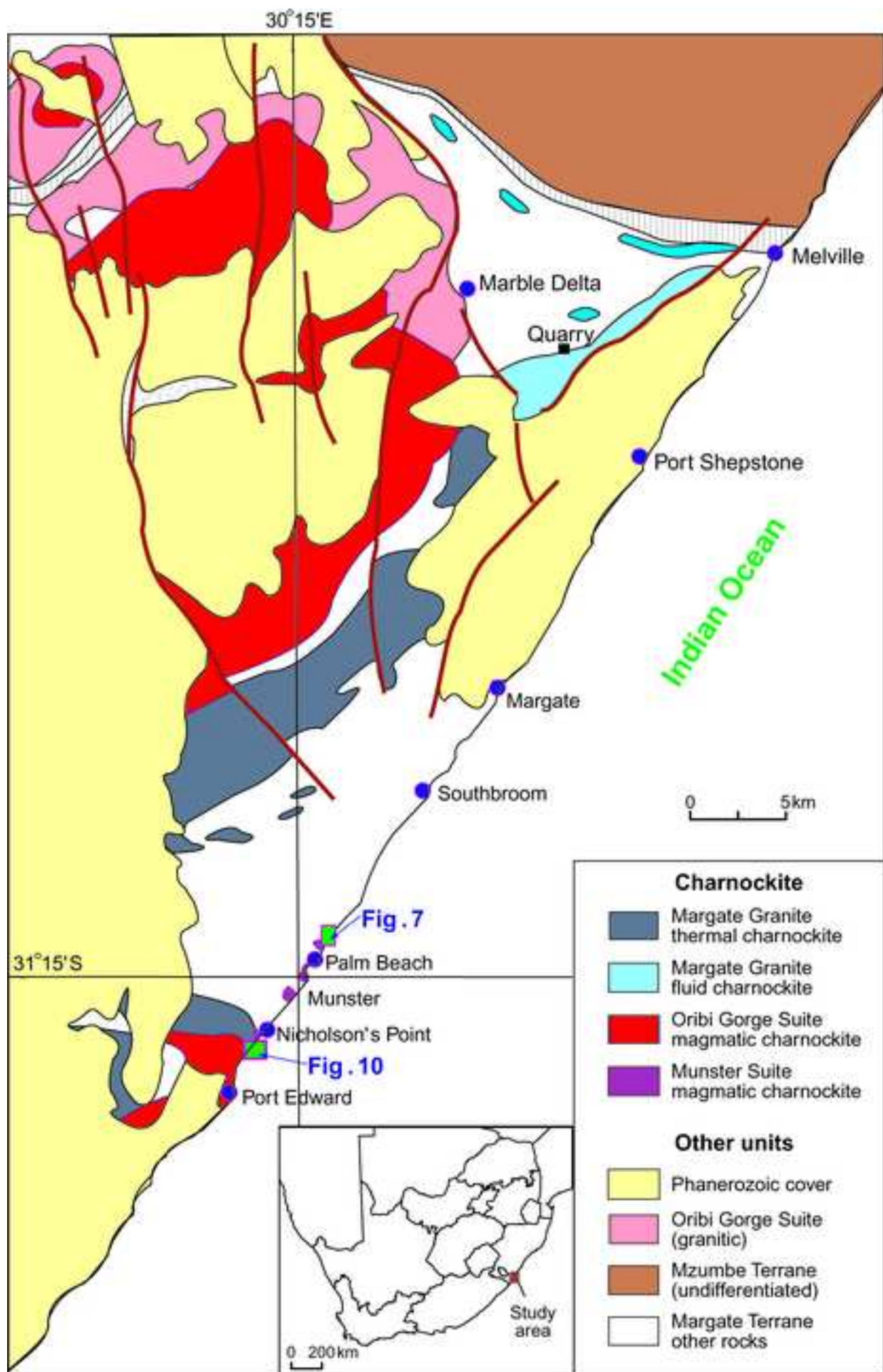


Figure 4

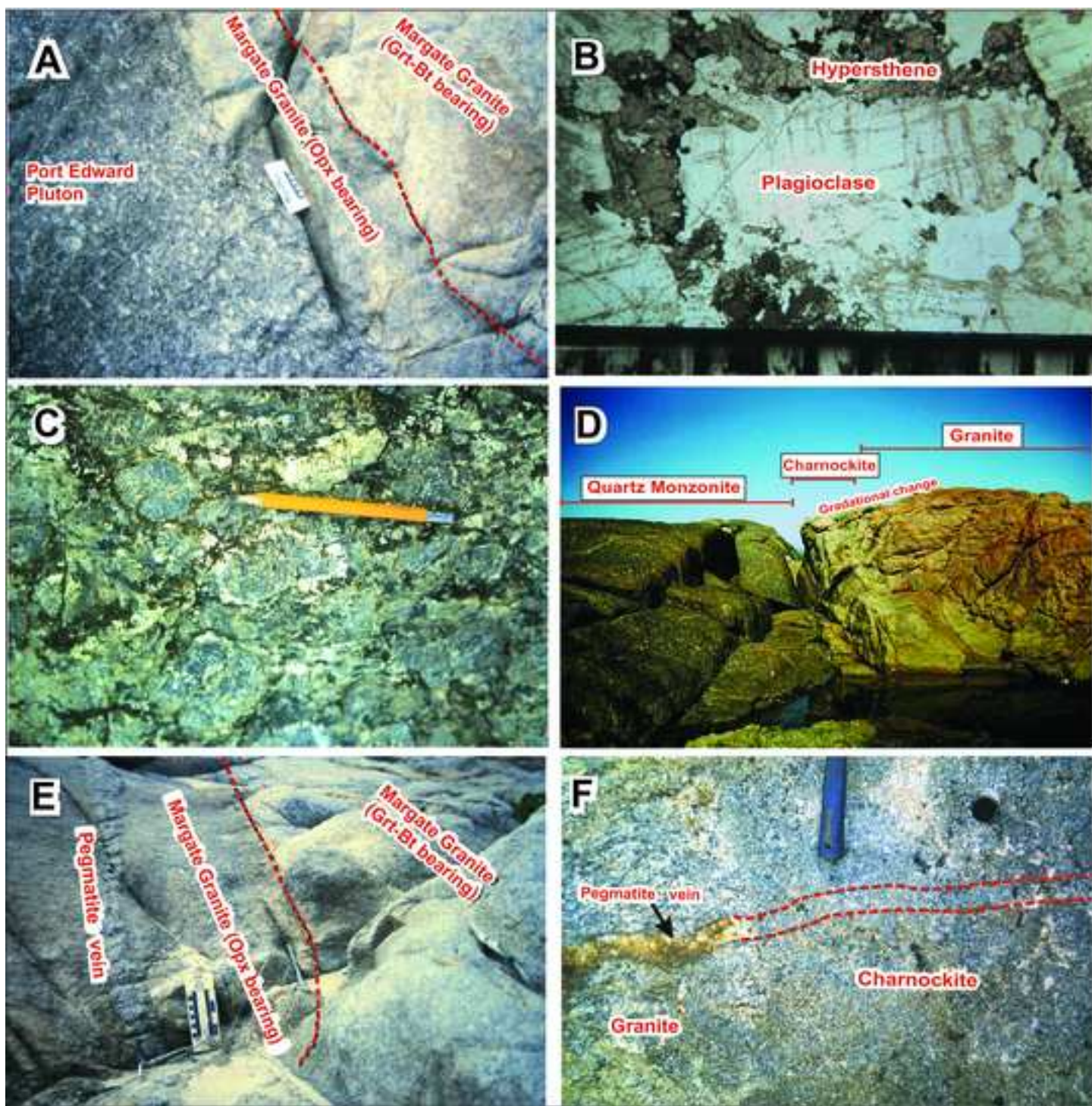
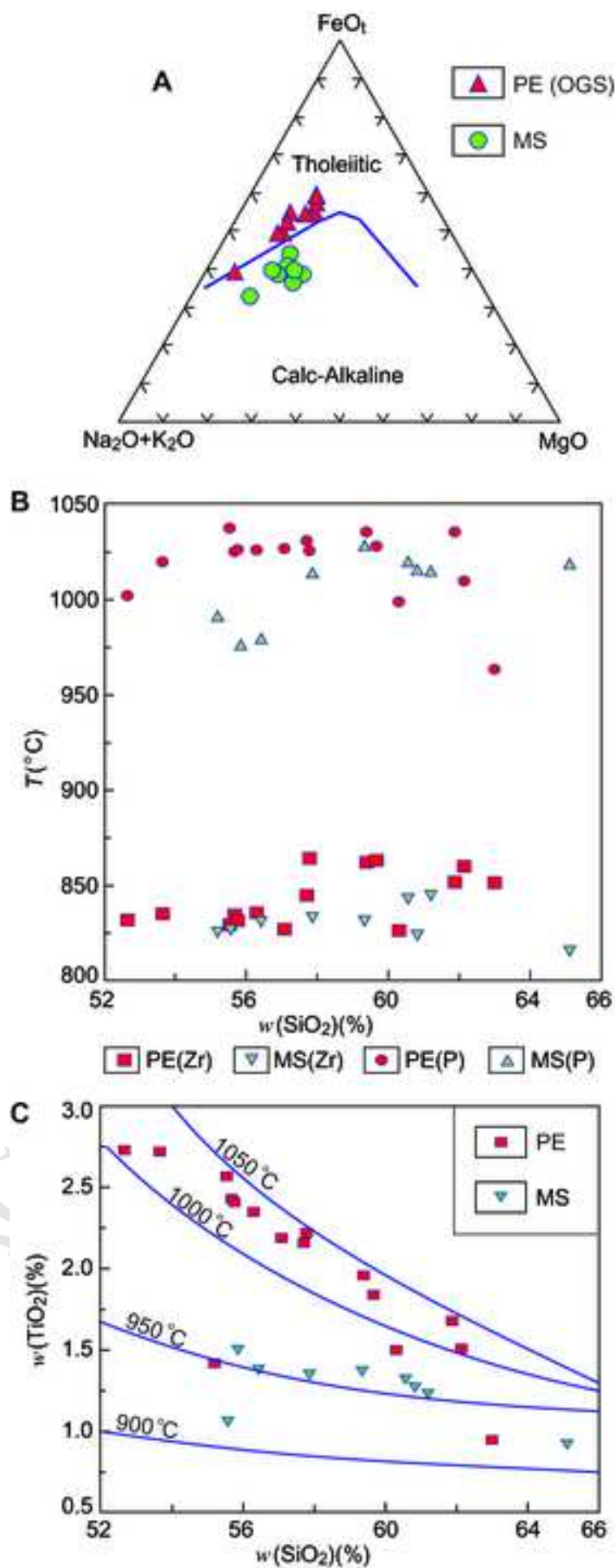


Figure 5

[Click here to download high resolution image](#) ACCEPTED MANUSCRIPT


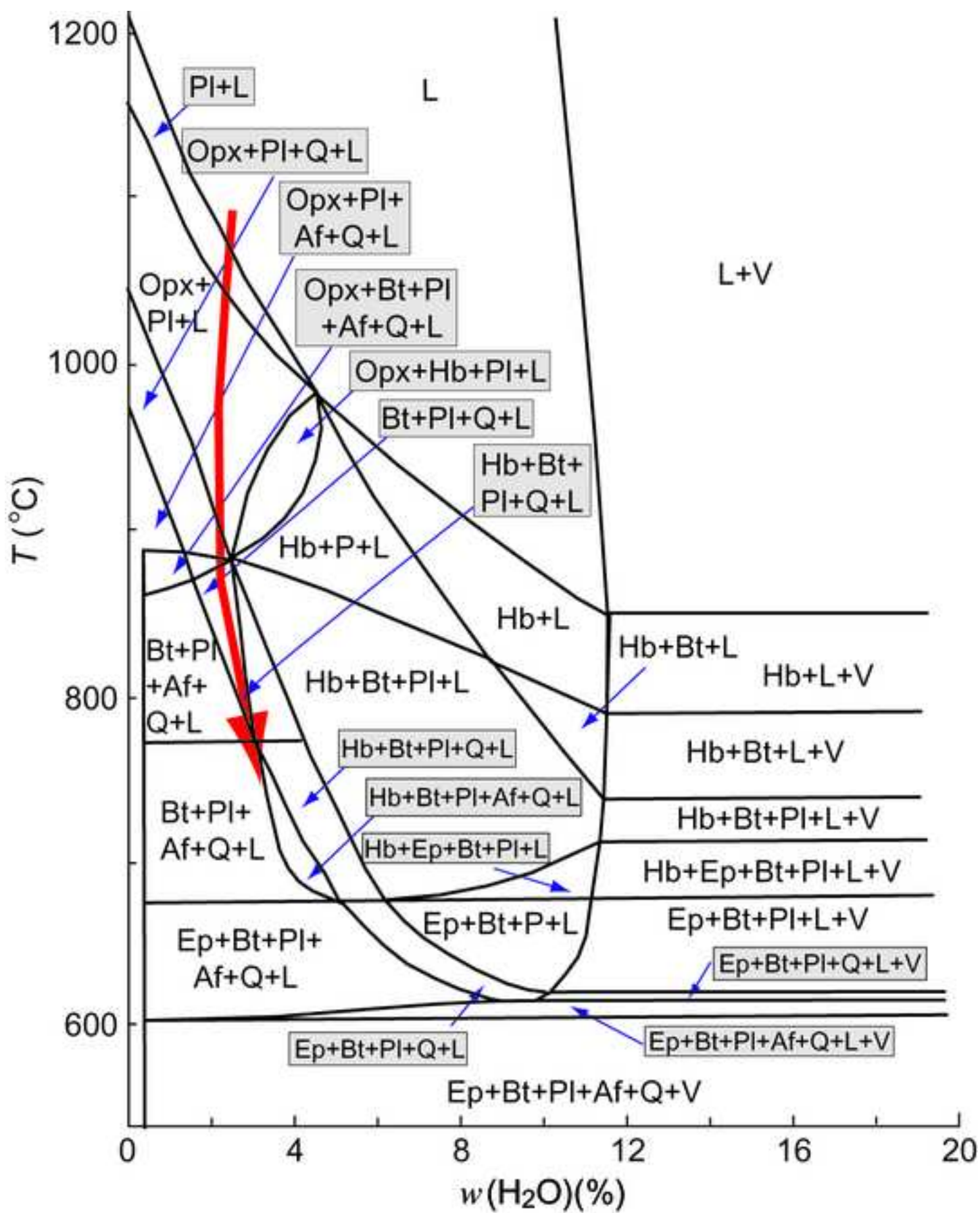




Figure 7

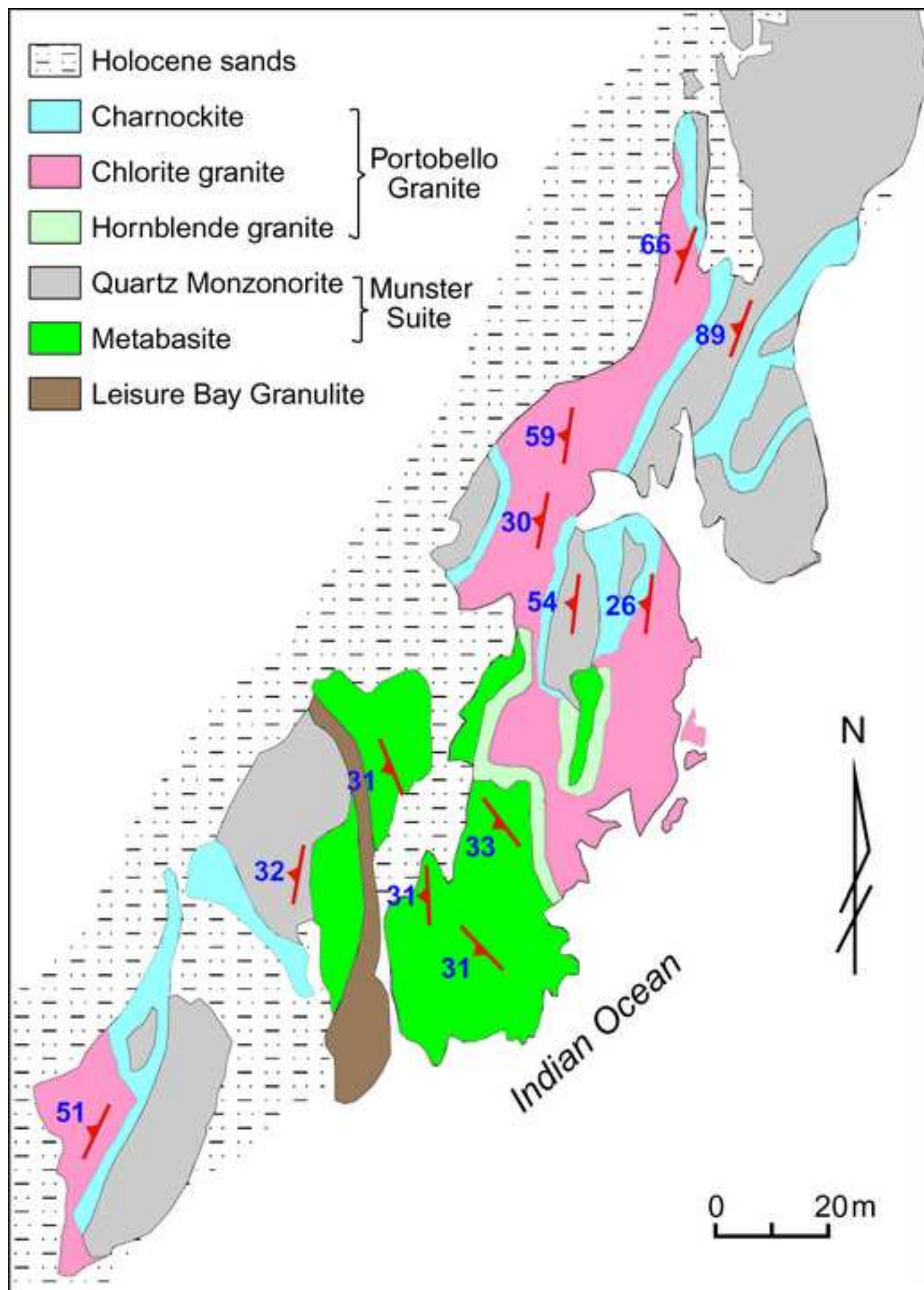


Figure 8

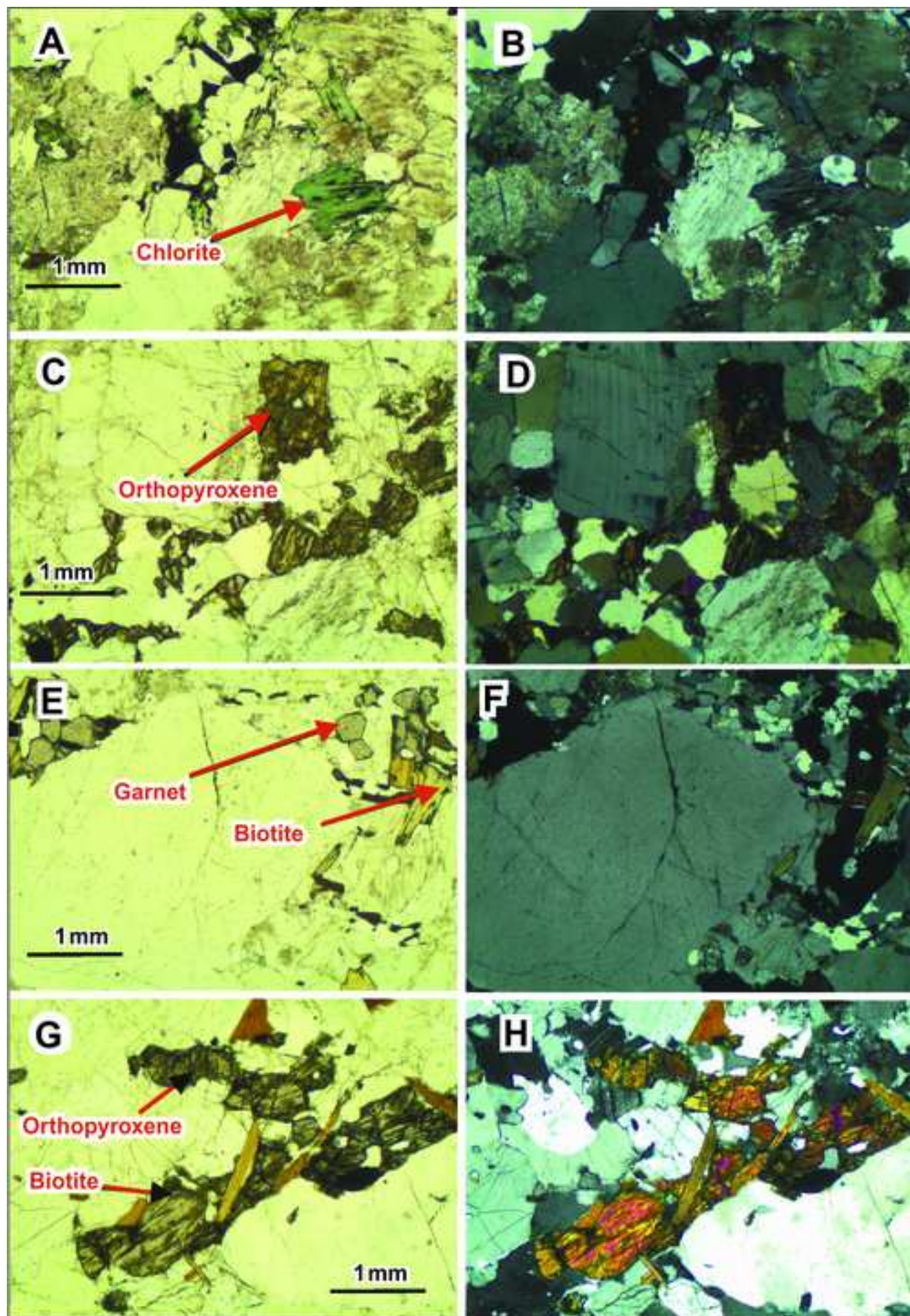


Figure 9

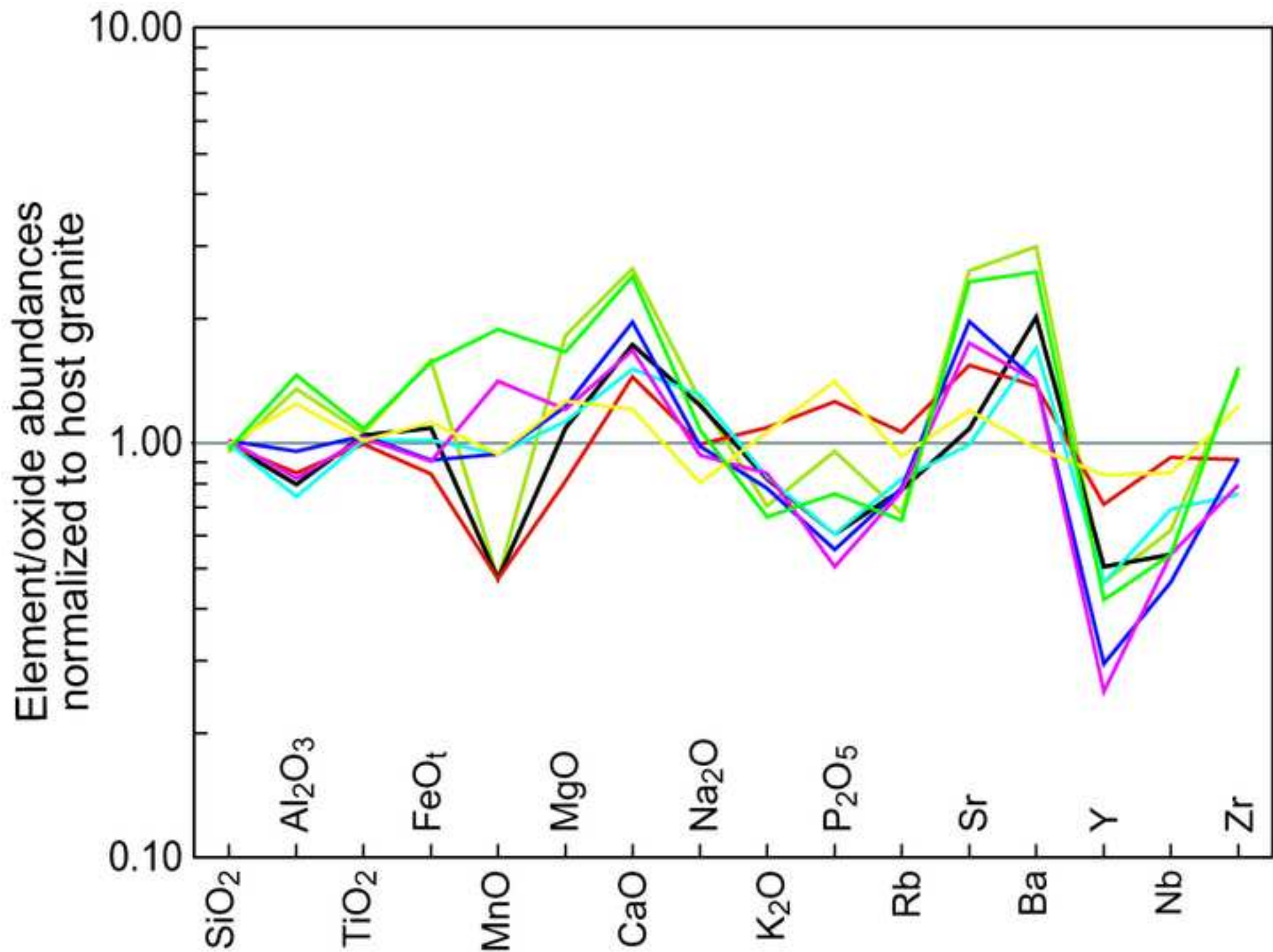


Figure 10

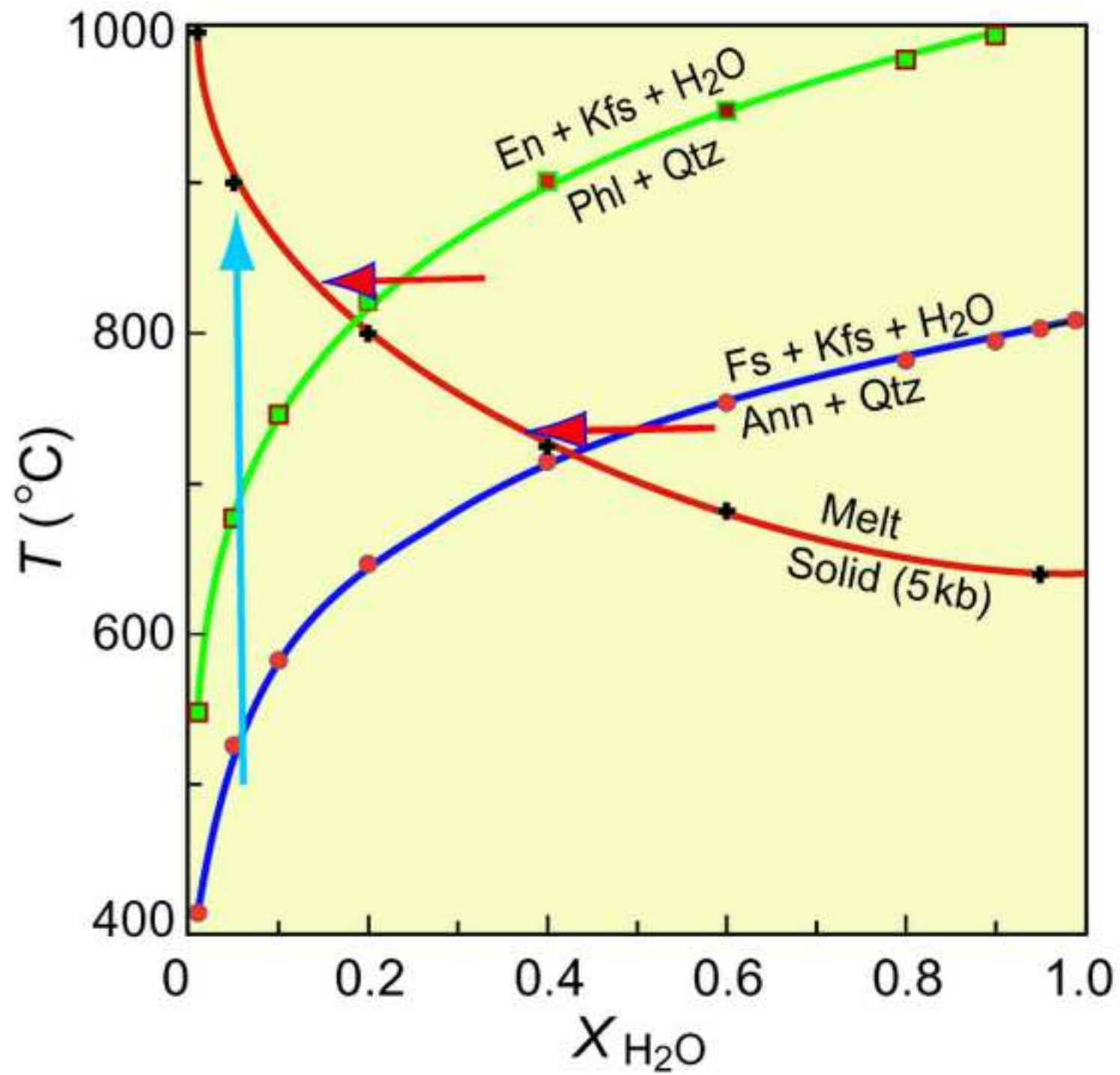
[Click here to download high resolution image](#)

Figure 11

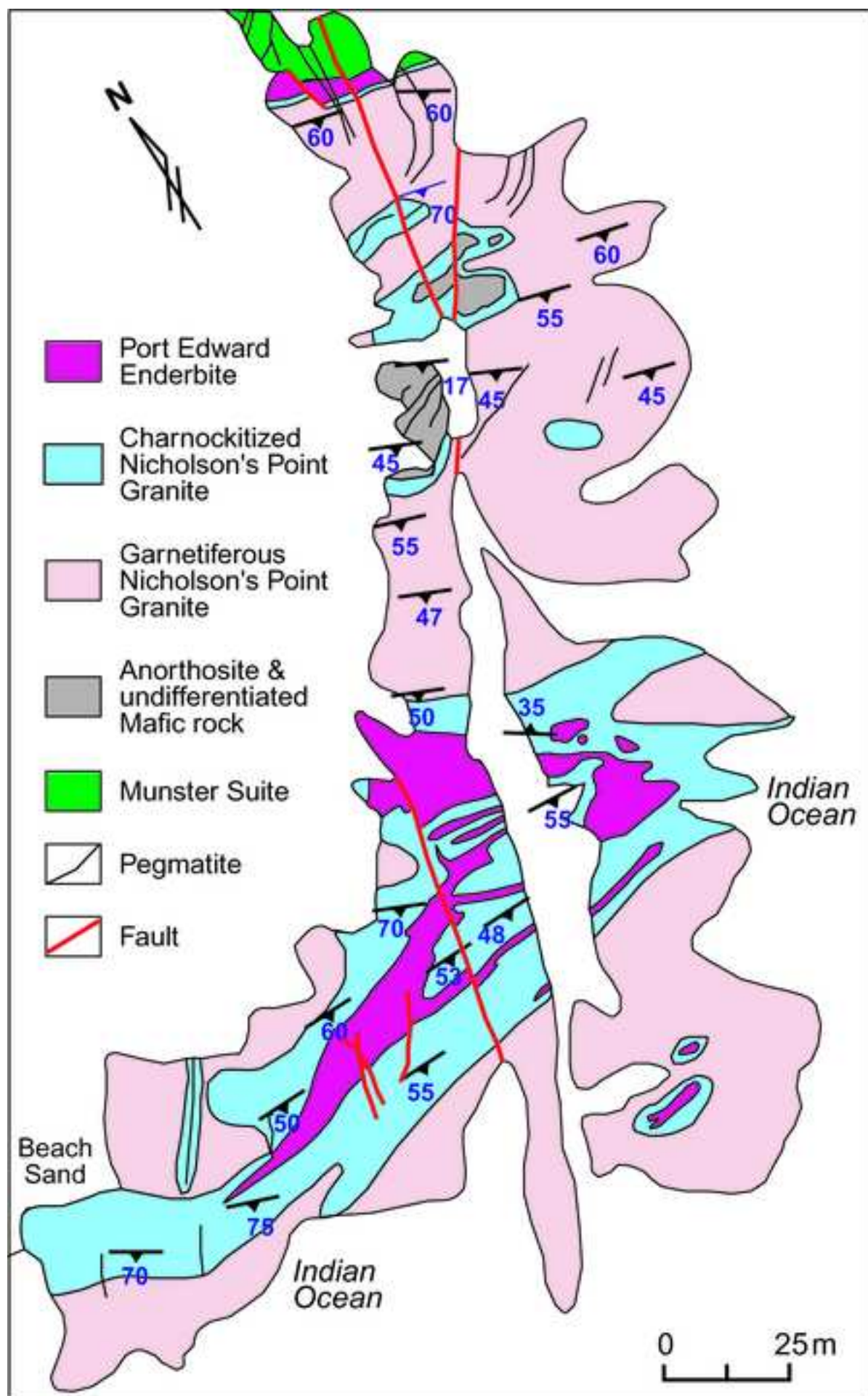


Figure 12

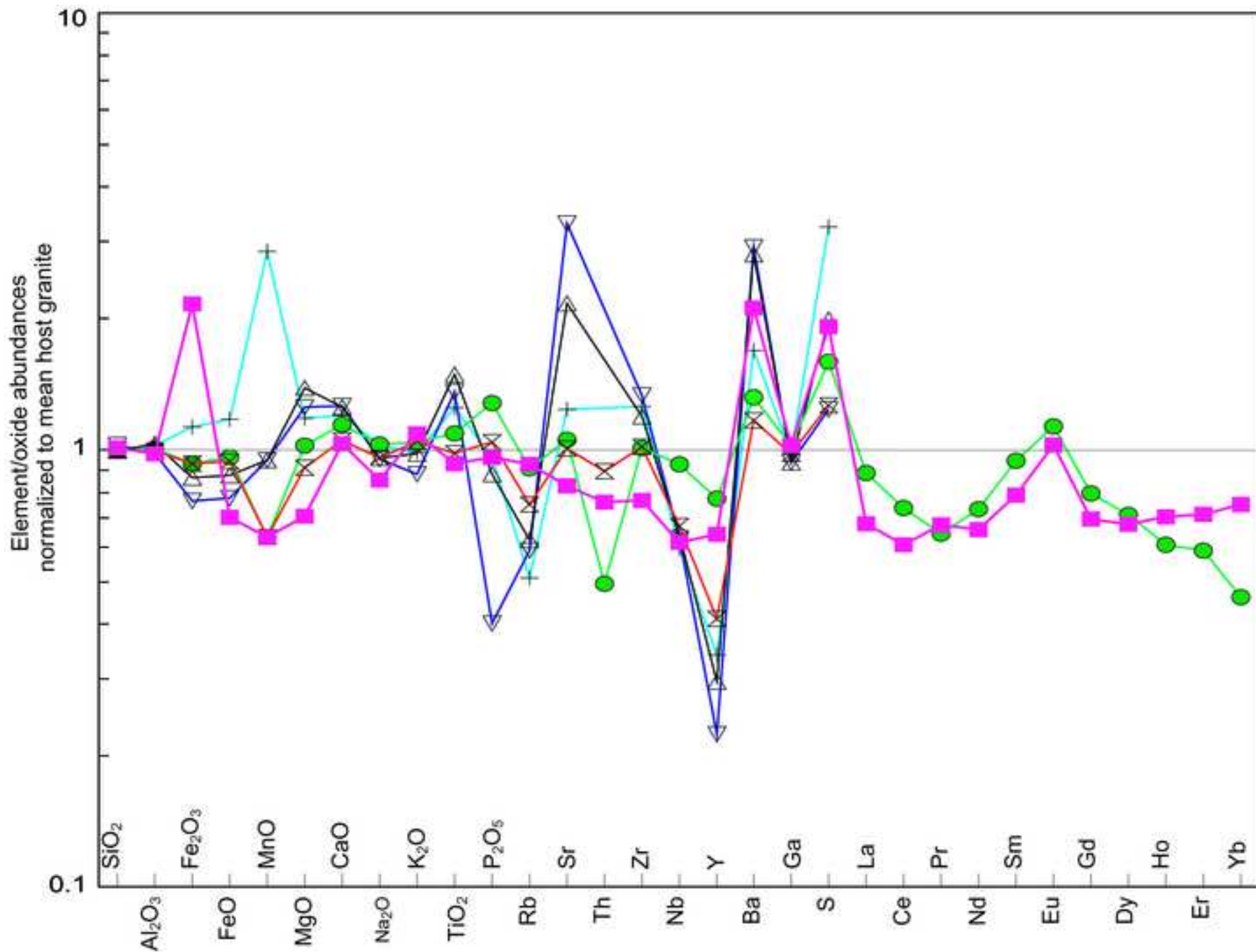
[Click here to download high resolution image](#)

Figure 13

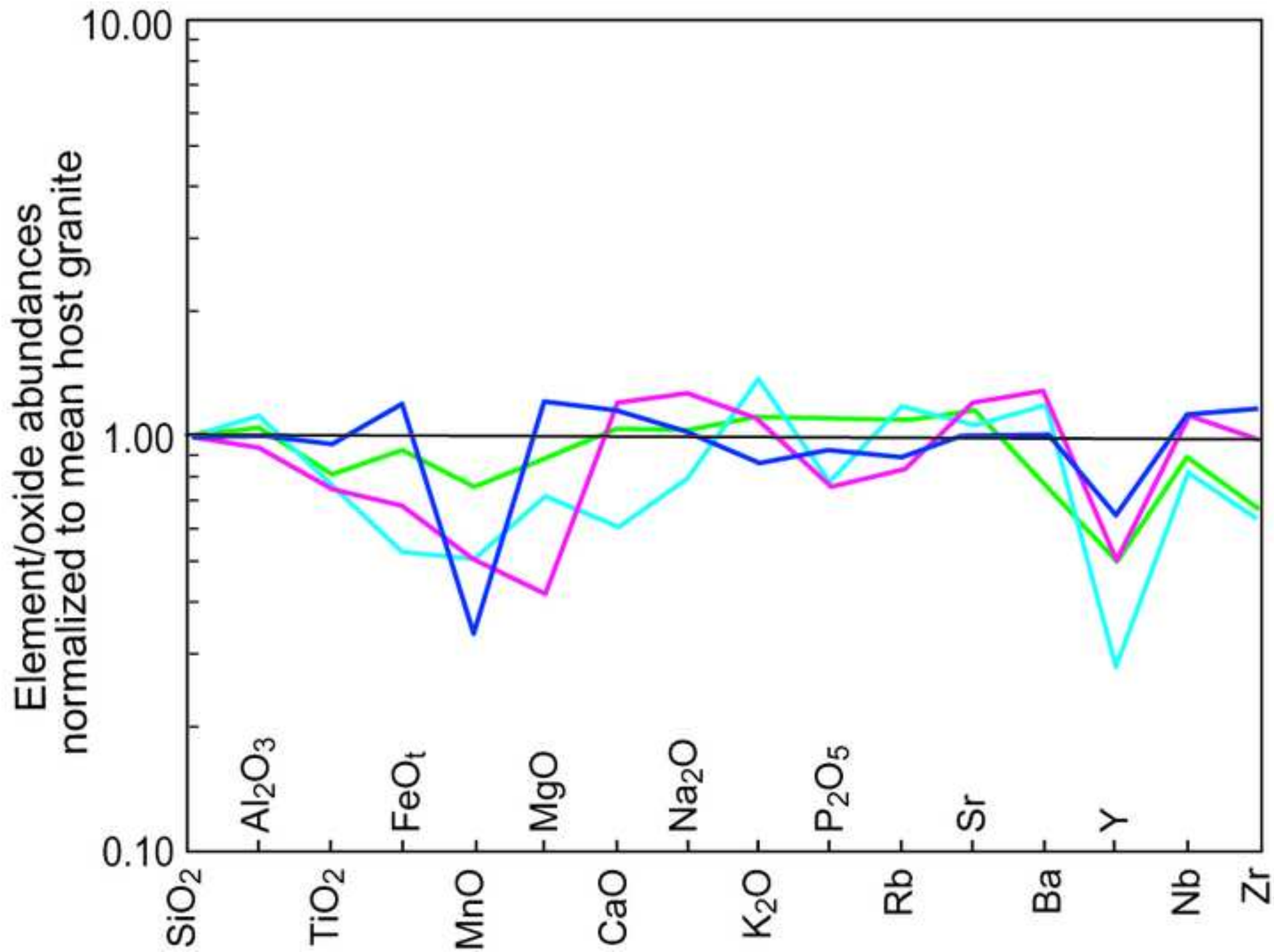
[Click here to download high resolution image](#)

Table 1 Major and trace element chemistry from the Port Edward pluton of the Oribi Gorge Suite. Major elements are in wt.% whereas trace elements are in ppm.

	GG75	GG67	GG71	GG74	UND4	UND3	GG83	RG5	UND2	UND5	UND1	RG4	GG85	GG97	GG86
SiO <sub>2</sub>	52.66	53.65	55.54	55.68	55.76	56.3	57.08	57.71	57.78	59.39	59.67	60.3	61.88	62.14	63
Al <sub>2</sub> O <sub>3</sub>	16.55	16.15	15.98	15.53	15.37	15.45	15.57	14.68	14.62	15.58	15.65	14.45	14.72	14.99	15.52
Fe <sub>2</sub> O <sub>3</sub>	2.59	2.46	2.38	2.46	2.45	2.39	2.39	2.40	2.34	2.18	2.13	2.46	1.88	1.93	1.85
FeO	9.21	9.58	8.47	8.67	8.62	8.30	7.77	7.74	8.07	7.15	6.95	6.81	6.08	6.28	4.48
MnO	0.18	0.18	0.17	0.17	0.17	0.15	0.15	0.11	0.15	0.13	0.13	0.13	0.11	0.12	0.09
MgO	3.08	3.10	2.71	2.60	2.53	2.46	2.42	2.24	2.23	2.00	1.89	2.17	1.66	2.06	1.38
CaO	6.53	6.57	5.80	6.00	5.95	5.77	5.68	5.28	5.26	4.88	4.90	3.65	4.78	4.21	3.23
Na <sub>2</sub> O	3.26	3.51	3.31	3.11	3.00	2.94	3.31	3.17	2.85	2.91	3.02	2.25	3.24	2.92	2.43
K <sub>2</sub> O	2.14	1.24	2.16	2.42	2.59	2.72	2.90	3.08	2.88	3.28	3.23	5.22	3.14	3.35	6.44
TiO <sub>2</sub>	2.73	2.72	2.57	2.43	2.41	2.35	2.19	2.16	2.22	1.96	1.84	1.50	1.68	1.51	0.95
P <sub>2</sub> O <sub>5</sub>	1.04	1.06	1.01	0.93	0.93	0.89	0.84	0.82	0.79	0.74	0.69	0.54	0.61	0.50	0.33
Total	99.97	100.22	100.10	100	99.78	99.72	100.30	99.39	99.19	100.20	100.10	99.48	99.78	100.01	99.70
Rb	53	25	42	43	52	55	58	74	55	69	72	117	68	71.8	144
Y	83	100	74	76	73	72	71	80	69	66	64	49	70	59.2	38
Nb	26	29	30	22	21	22	19	22	23	20	20	14	18	18.7	8
Sc	30	35	29	33	29	29	24	29	27	26	21	24	25	24	19
La	69	66	65	59	57	66	66	77	68	64	66	25	78	65.1	40
V	128	131	118	111	110	110	100	96	102	90	85	105	86	80.1	56
Sr	429	478	548	509	499	478	527	442	446	456	429	512	406	322	487
Zr	572	572	479	544	528	522	499	595	666	565	572	376	534	495	455
Ba	1184	483	1178	1343	1187	999	1337	1153	1115	1179	1106	2671	1065	1111	2247
Cr	24	29	58	21	17	52	19	47	17	16	12	39	28	37.9	8
Cu	10	13	10	14	13	12	11	13	11	9	9	8	8	10.7	37
Ni	10	9	21	9	6	15	7	14	5	6.6	4	5	8	12	9
Zn	193	197	187	180	177	180	157	161	177	157	155	153	142	131	103



1

Table 2 Tabulation of data from the stable isotope analysis of fluids released during decrepitation experiments on samples from the Port Edward pluton and Oribi Gorge plutons of the Oribi Gorge Suite.

Results showing the carbon isotopic composition of fluid inclusions in charnockites					
Sample Nos.	Sample type	Decrepitation temperature (°C)	CO <sub>2</sub> gas released (mmol/g)	$\delta^{13}\text{C}_{\text{PDB}}$	1 $\sigma$
GG-67 (Port Edward pluton)	Quartz	800	19.30	-7.99	0.03
	Whole rock	800	25.70	-6.82	0.02
	Whole rock	1000	38.42	-9.72	0.03
	Whole rock + V <sub>2</sub> O <sub>5</sub>	1000	34.17	-10.15	0.01
UM-2 (Oribi Gorge pluton)	Quartz	800	6.97	-1.1	0.04
	Whole rock	800	14.51	-5.61	0.01
	Whole rock	1000	15.83	-6.15	0.01
	Whole rock + V <sub>2</sub> O <sub>5</sub>	1000	16.39	-6.94	0.02

1

Table 3 Major and trace element chemistry from the Portobello granite. Major elements are in wt.% whereas trace elements are in

	Charnockite								Pink granite							
	PB1	PB2	PB3	PB4	PB11	PB13	PB14	PB16	PB5	PB6	PB7	PB8	PB15	PB12	PB17	PB18
SiO <sub>2</sub>	68.12	71.22	71.17	71.43	72.66	72.83	70.99	69.33	71.94	70.93	71.67	70.46	72.19	73.15	71.60	71.96
Al <sub>2</sub> O <sub>3</sub>	14.59	14.40	13.72	14.01	14.36	14.17	14.02	14.95	13.15	13.63	13.93	14.51	13.82	13.82	13.69	13.82
Fe <sub>2</sub> O <sub>3</sub>	3.21	2.20	1.71	2.06	1.84	1.83	2.27	3.17	1.90	2.16	1.88	2.11	1.98	1.75	2.21	2.22
FeO	0.40	0.27	0.21	0.25	0.23	0.23	0.28	0.39	0.24	0.27	0.23	0.26	0.24	0.22	0.27	0.27
MnO	0.01	0.01	0.01	0.02	0.02	0.03	0.02	0.04	0.02	0.03	0.01	0.02	0.02	0.02	0.02	0.03
MgO	0.92	0.55	0.41	0.57	0.62	0.61	0.64	0.84	0.53	0.54	0.50	0.56	0.48	0.42	0.52	0.50
CaO	2.64	1.73	1.45	1.51	1.96	1.68	1.21	2.53	0.86	1.11	1.12	0.81	0.98	1.05	1.19	0.90
Na <sub>2</sub> O	3.53	3.44	2.77	3.64	2.74	2.61	2.24	3.00	3.49	3.08	3.09	3.63	2.20	2.38	2.13	2.33
K <sub>2</sub> O	4.20	4.88	6.50	4.93	4.64	5.04	6.34	3.95	5.36	6.06	5.88	5.60	6.31	6.03	6.23	6.24
TiO <sub>2</sub>	0.51	0.30	0.32	0.28	0.36	0.31	0.47	0.55	0.40	0.34	0.38	0.40	0.39	0.28	0.43	0.40
P <sub>2</sub> O <sub>5</sub>	0.19	0.12	0.25	0.12	0.11	0.10	0.28	0.15	0.16	0.23	0.22	0.23	0.19	0.13	0.23	0.20
LOI	1.10	0.73	0.01	0.56	0.12	0.22	0.46	0.38	1.22	1.12	0.88	0.97	0.56	0.39	0.64	0.68
Total	99.41	99.85	98.53	99.38	99.66	99.66	99.22	99.28	99.27	99.50	99.79	99.56	99.36	99.64	99.16	99.55
Rb	130	148	204	157	149	147	178	125	173	212	181	208	174	183	201	203
Sr	499	208	296	190	377	334	230	469	284	131	267	221	188	162	152	130
Ba	1779	1204	820	1014	843	842	582	1546	785	501	686	705	532	605	517	451
Y	11	12	17	11	7	6	20	10	17	27	23	27	15	14	25	43
Nb	8	7	12	9	6	7	11	7	15	12	15	15	11	9	13	14
Zr	397	213	245	202	246	213	329	410	302	261	271	284	274	187	299	274
Sc	9	5	5	4	4	4	4	6	6	4	8	5	3	3	3	3
Ga	20	18	20	19	20	19	20	21	18	16	19	21	19	20	21	20
V	30	16	7	13	38	32	39	55	17	10	13	13	34	27	40	35
Cu	11	8	10	7	5	5	6	5	7	9	8	9	7	5	5	5
Ni	3	5	3	6	5	5	5	5	7	3	3	3	5	5	5	5
Zn	56	48	30	41	41	36	50	62	36	45	37	44	39	40	53	41

ppm.